

NASA  
CR  
3507  
c.1

NASA Contractor Report 3507



# CAS22 – FORTRAN Program for Fast Design and Analysis of Shock-Free Airfoil Cascades Using Fictitious-Gas Concept

Djordje S. Dulikravich and Helmut Sobieczky

LOAN COPY: RETURN TO  
AFWL TECHNICAL LIBRARY  
KIRTLAND AFB, NM.

CONTRACT NAS3-22532  
JANUARY 1982

**NASA**



NASA Contractor Report 3507

**CAS22 – FORTRAN Program  
for Fast Design and Analysis  
of Shock-Free Airfoil Cascades  
Using Fictitious-Gas Concept**

Djordje S. Dulikravich  
*Universities Space Research Association  
Columbia, Maryland*

Helmut Sobieczky  
*DFVLR—Institute für Theoretische Stroemungsmechanik,  
Goettingen, Federal Republic of Germany*

Prepared for  
Lewis Research Center  
under Contract NAS3-22532



National Aeronautics  
and Space Administration

**Scientific and Technical  
Information Branch**

1982

CAS22 - Fortran Program for Fast Design and Analysis of Shock-Free  
Airfoil Cascades Using Fictitious-Gas Concept

by Djordje S. Dulikravich\* and Helmut Sobieczky\*\*

SUMMARY

A user-oriented computer program, CAS22, was developed that is applicable to aerodynamic analysis and transonic shock-free redesign of existing two-dimensional cascades of airfoils. CAS22 can be used in three separate modes of operation: (1) as an analysis code for full-potential, transonic, shocked or shock-free cascade flows, (2) as a design code for shock-free cascades that uses Sobieczky's fictitious-gas concept, and (3) as a shock-free design code followed automatically by the analysis in order to confirm that the newly obtained cascade shape provides for an entirely shock-free transonic flow field. CAS22 generates its own four-level, boundary-conforming grid of an O type.

The mathematical model of the flow is a full-potential equation. Its artificially time-dependent form is solved in a fully conservative form by using a finite area technique; rotated, type-dependent upstream differencing; and successive line over relaxation.

Isentropic shocks are captured by using a first-order artificial viscosity in fully conservative form. The shock-free design is performed by implementing Sobieczky's fictitious-gas concept of elliptic continuation from subsonic into supersonic flow domains. Recomputation inside each supersonic zone is performed by the method of characteristics in the rheograph plane by using isentropic gas relations. The new shock-free contour is determined from the condition that stream function is equal to zero on the airfoil surface. Besides being capable of converting existing cascade shapes with multiple shocked supersonic regions into shock-free cascades, CAS22 can also unchoke previously choked cascades and make them shock free.

---

\*Visiting Research Scientist at NASA Lewis Research Center presently employed by the Universities Space Research Association, Columbia, Maryland.

\*\*Research Scientist, DFVLR - Institute für Theoretische Strömungsmechanik, Goettingen, Federal Republic of Germany.

## INTRODUCTION

Transonic flow is characterized by the coexistence of subsonic and supersonic local flow domains. These supersonic regions generally terminate with shocks, which are the main generators of vorticity and entropy. As a consequence the aerodynamic drag force (wave drag) and the aerodynamic noise level increase sharply, and this results in a rapid decay of the aerodynamic efficiency of the cascade. When the shocks are strong enough, the shock - boundary layer interaction leads to boundary layer separation and potentially dangerous unsteady flow and mechanical vibrations.

Besides these general features, transonic flow through the cascades of airfoils is often characterized by the flow-choking phenomenon. Choking occurs when two neighboring airfoils in a cascade are connected by a single sonic line. Choking places an upper limit on the mass flow through a given cascade. It inevitably occurs in accelerated turbine cascade flows with supersonic exit conditions.

For shock-free or shockless flow the fluid decelerates from supersonic speed to subsonic speed not discontinuously (shocked flow) but smoothly over a finite distance (isentropic recompression). There are only a limited number of design techniques for obtaining shock-free cascade flows. The method of complex characteristics developed by Garabedian (refs. 1 and 2) and applied to cascade design by Garabedian and Korn (ref. 3) is probably the most mathematically rigorous and complex technique presently in use by industry (ref. 4). This method was proven to work well in the design of high-performance isolated airfoils and cascades. It gives the designer a freedom to prescribe velocity distribution along the entire (yet unknown) contour of an airfoil in the cascade. The result is an entirely shock-free flow field and a cascade shape compatible with this flow field. The main drawbacks of this technique are that very often the input surface velocity distribution is unrealistic and the resulting cascade shape does not have any physical meaning. This technique cannot be applied to three dimensions, and for the design of practically interesting shock-free planar cascades this technique requires a significant amount of user experience. An original and instructive technique for designing shock-free cascades of airfoils by using electrical analog was developed by Sobieczky (ref. 5). Because of its complex hardware requirements this unique technique has not found wide acceptance in industry.

A relatively simple method based on the hodograph transformation was developed by Schmidt (ref. 6). It is fast and easy to understand, but it has a significant drawback associated with its stream function formulation. The resulting cascade shapes appear to have only sharp leading and trailing edges. As a consequence, the designer is forced to somewhat arbitrarily round these edges at the expense of the expected aerodynamic performance of the cascade.

Yet another technique for designing shock-free cascade flows is presented in this report. It is based on the fictitious-gas concept of Sobieczky (ref. 7) and the full-potential, steady, transonic cascade analysis code of Dulikravich (ref. 8). The present work has two main objectives. One is to eliminate all shocks from the flow field. The other is to unchoke already choked cascades and to make them shock free.

Both tasks will be achieved by partially reshaping ("shaving off") existing airfoil shapes in a cascade without changing their stagger angle, chord length, or gap-chord ratio.

These goals seemed (ref. 9 and private communication with P. Garabedian, Courant Institute of Mathematics, New York University) to be accomplishable by prescribing a smooth, shock-free surface pressure distribution along a portion of a given airfoil

and of velocity profiles measured at NASA Lewis Research Center (presently employed by the University of Maryland, Baltimore County, Maryland).  
Researcher, Federal Republic of Germany.

contour and then determining a partially new airfoil shape that is consistent with the prescribed surface pressure distribution. Because of the highly nonlinear character of the transonic flow this design technique generally does not create an entirely shock-free flow field.

It has been suggested in a number of standard textbooks on gas dynamics (ref. 10) and accidentally observed (private communication with J. McFagen,) that a number of shocks can remain in the flow field although each airfoil surface is shock free. These shocks have the unique property of terminating before reaching an airfoil surface. The conclusion is that an entirely shock-free flow field cannot be obtained solely by prescribing shock-free surface pressure without enforcing shock-free conditions throughout the flow field.

All these techniques were developed with a specific goal to create an entirely shock-free cascade flow field for a single set of global flow and geometric parameters. For this purpose a shock-free surface pressure prescription technique alone cannot be accepted as appropriate.

### Fictitious-Gas Concept

For the specific purpose of designing shock-free transonic flow fields Sobieczky developed (ref. 7), elaborated (ref. 11), and successfully applied (ref. 12) the idea of a fictitious-gas elliptic continuation. This truly ingenious concept is easy to understand and to apply, yet it is mathematically and physically sound and correct. The method consists of three basic steps. The first step is an iterative determination of the shape of a sonic line bounding a supersonic shock-free flow domain. This is attained by utilizing nonphysical (fictitious) expressions for the fluid density and the speed of sound whenever the flow is locally supersonic.

The second step of the design procedure recomputes the flow field inside that supersonic domain by using now physical (isentropic) relations for the fluid density and the speed of sound. The third step then searches through this supersonic domain for the points where stream function has a zero value and thus determines a shock-free airfoil shape that differs from the input airfoil contour only along the section wetted by the supersonic shock-free flow. Computer program CAS22 unifies all three steps of the design procedure.

Step 1 - The continuity equation for a steady, compressible flow normalized by the critical values

$$\vec{\nabla} \cdot \left( \frac{\rho}{\rho_*} \frac{q}{q_*} \right) = \left( \frac{\rho}{\rho_*} \frac{u}{q_*} \right)_{,x} + \left( \frac{\rho}{\rho_*} \frac{v}{q_*} \right)_{,y} = 0 \quad (1)$$

can be expressed in its canonical full-potential form (ref. 13) as

$$\frac{\rho}{\rho_*} \left( (1 - M_*^2) \phi_{,ss} + \phi_{,nn} \right) = 0 \quad (2)$$

Here  $\rho$  is the density,  $u$  and  $v$  are the velocity vector components along the  $x$  and  $y$  coordinate axes correspondingly,  $M_*$  is the local critical Mach number,  $s$  is the local streamline aligned coordinate and  $n$  is the coordinate, locally orthogonal on the streamline. When the flow is locally subsonic ( $M_* < 1$ ),

equation (2) is a nonlinear but elliptic. This means that the mass flow ( $\rho q / \rho_* q_*$ ) will continue to increase with increasing of  $M_*$  until the critical flow conditions are met (fig. 1). This can be concluded from the expression for mass conservation

$$\frac{q}{q_*} \frac{\rho}{\rho_*} = M_* \frac{\rho}{\rho_*} \quad (3)$$

For an isentropic flow we can write

$$\frac{\rho}{\rho_*} = \left( \frac{\gamma + 1}{2} - \frac{\gamma - 1}{2} M_*^2 \right)^{\frac{1}{\gamma - 1}} \quad (4)$$

and

$$a^2 / a_*^2 = (\rho / \rho_*)^{\gamma - 1}$$

where  $\gamma$  is a specific heat ratio of a calorically perfect gas. Equation (3) has a maximum value of 1 when  $M_* = 1$ . Once the flow field becomes locally supersonic ( $M_* > 1$ ), equation (2) changes its type and becomes nonlinear and hyperbolic. With the further increase of  $M_*$ , mass flow will start to decrease. Supersonic flows generally revert to subsonic conditions discontinuously through a shock wave (or an isentropic discontinuity in the case of a full-potential flow model). To prevent this from ever happening, each time when the flow is locally supersonic ( $M_* > 1$ ) a fictitious-gas relation should be introduced so that the governing equation (2) continues to retain its elliptic character (ref. 14).

This must be done in such a way that the mass flow never decreases after it reaches its physically maximum value of 1. Hence, the parabolicity condition (refs. 15 and 16) for any fictitious gas is

$$\frac{\rho_f}{\rho_*} \geq \frac{1}{M_*} ; \quad M_* \geq 1 \quad (6)$$

That is, isentropic and fictitious-gas relations should coincide only along the sonic line where  $M_* = 1$ . Recently, professor David Caughey of Cornell University pointed out an additional general constraint which every fictitious gas relation should satisfy. Namely, the slope of any fictitious density curve (fig. 2) must be less than the slope of the parabolic low density curve for any value of  $M_*$  greater than one.

$$\frac{d}{dM_*} \left( \frac{\rho_f}{\rho_*} \right) > \frac{d}{dM_*} \left( \frac{\rho}{\rho_*} \right) \quad (7)$$

In addition, an analytic expression for the fictitious mass flow should have the same slope as the isentropic mass flow formula at  $M_* = 1$ ; that is,

$$\frac{d}{dM_*} \left( M_* \frac{\rho}{\rho_*} \right) = \frac{d}{dM_*} \left( M_* \frac{\rho_f}{\rho_*} \right) = 0 \quad (8)$$

or

$$\frac{\rho_f}{\rho_*} + M_* \frac{d}{dM_*} \left( \frac{\rho_f}{\rho_*} \right) = 0 \quad (9)$$

When  $M_* = 1$ , it becomes

$$\frac{d}{dM_*} \left( \frac{\rho_f}{\rho_*} \right) = -1 \quad (10)$$

From the general continuity criterion (refs. 16 and 17) one easily obtains a general formula for the fictitious speed of sound normalized with the critical speed of sound as

$$\frac{a_f^2}{a_*^2} = -M_* \left( \frac{\rho_f}{\rho_*} \right) \frac{1}{\frac{d}{dM_*} \left( \frac{\rho_f}{\rho_*} \right)} \quad (11)$$

For all practical purposes there is an infinity of choices for the analytic expression of fictitious density and fictitious speed of sound that all fulfill the conditions expressed in equations (6), (7), and (10). The main decisive factor should be the economy and speed of numerical evaluation of both fictitious quantities. When choosing a simple expression for  $\rho_f/\rho_*$ , we must keep in mind that it should produce an equally simple expression for  $a_f^2/a_*^2$ .

In the CAS22 program a simple parabolic-law expression was used

$$P \left( \frac{\rho_f}{\rho_*} - 1 \right)^2 - \left( \frac{\rho_f}{\rho_*} - 1 \right) - (M_* - 1) = 0 \quad (12)$$

which gives (ref. 16)

$$\frac{\rho_f}{\rho_*} = 1 + \frac{1 - \sqrt{1 + 4P(M_* - 1)}}{2P} \quad (13)$$

and (from eq. (11))

$$\frac{a_f^2}{a_*^2} = M_* \left( 1 + \frac{1 - \sqrt{1 + 4P(M_* - 1)}}{2P} \right) \sqrt{1 + 4P(M_* - 1)} \quad (14)$$

A single constant input parameter  $P$  has the purpose of making the fictitious gas more or less incompressible (fig. 2). This translates into the physical fact of how much longer and flatter the resulting supersonic shock-free flow domain will be than the original shocked supersonic zone (fig. 3).

As already stated, the fictitious-gas relations are used during the iterative solution of the full-potential equation only at the grid points that indicate locally supersonic flow. This means that once the iterative procedure converges, the subsonic part of the flow field and the sonic lines will be correctly calculated from equations (1), (4) and (5). Hence lift and drag coefficients will be correctly determined, and the subsequent recomputation of the supersonic domains will not change them. Note that these coefficients will correspond to the new shock-free cascade shape to be determined by design steps 2 and 3. These coefficients will differ from the coefficients of lift and drag that were obtained for the original shocked cascade by using isentropic relations only.

The main drawback of the fictitious-gas concept as used in this work is that the user cannot prescribe the specific form of the shock-free surface pressure distribution. The only thing that he can prescribe is the value of the constant  $P$  in equations (13) and (14) that will guarantee an entirely shock-free flow field. The resulting airfoil surface shock-free pressure distribution cannot be quantitatively influenced in a controlled fashion.

It can be concluded now that the fictitious-gas technique should be used for redesigning the existing transonic cascades and making them shock free. The fictitious-gas concept is not limited in its application only to two-dimensional planar problems as are hodograph techniques; it has been successfully applied to both arbitrary two-dimensional (ref. 15) and three-dimensional (ref. 18) configurations.

Step 2. - After the iterative process for numerically solving the full-potential equation has converged, the entire flow field is searched for the location of sonic lines. CAS22 is capable of accurately determining the shapes of an arbitrary number of supersonic shock-free regions. It is not capable in its present version of detecting the shape of a choking sonic line obtained from the fictitious-gas computations. CAS22 can calculate flows where the leading edge can be covered completely by the supersonic flow, but trailing edge must be subsonic. Once the  $x^*$ ,  $y^*$  coordinates of a sonic line enveloping the particular supersonic zone are found by interpolation, values of the velocity vector components  $u^*/a^*$  and  $v^*/a^*$  are determined together with the values of the velocity potential function  $\phi^*$ .

Values of the stream function  $\psi^*$  along the sonic line are then determined by numerically integrating

$$d\psi^* = ay^* \cos \theta^* - dx^* \sin \theta^* \quad (15)$$

where



$$\theta^* = \tan^{-1} \left( \frac{v^*}{u^*} \right) \quad (16)$$

is the local flow angle on the sonic line. Thus we obtained all the necessary data along the sonic line. These data will serve as initial data for the two-dimensional, method-of-characteristics marching integration (recomputation) of the full-potential equation inside the supersonic zone, where now only isentropic relations are used (ref. 7). The method of characteristics was used because it represents the most accurate, fastest, and simplest technique for integrating hyperbolic partial differential equations. The fact that we are integrating a quasi-linear hyperbolic equation is circumvented by rewriting the full-potential equation in its rheograph form (ref. 7).

$$\phi_{,v} = K(v) \psi_{,\theta} \quad (17)$$

$$\phi_{,\theta} = K(v) \psi_{,v}$$

Note that in the rheograph plane (local flow angle  $\theta$  versus Prandtl-Meyer function  $v(M^*)$ ) the hyperbolic, quasi-linear, full-potential equation becomes linear. It is valid inside the triangular domain (fig. 4) bordered by the sonic line data ( $v^* = 0$ ;  $\theta_A^* \leq \theta^* \leq \theta_B^*$ ) and the end characteristics  $\xi = \text{constant}$  and  $\eta = \text{constant}$ , which are mutually orthogonal. Numerical integration of equation (17) can be easily performed inside the entire triangle ABC in the hodograph plane if the characteristic grid is uniform (fig. 4). This is the case only if the total flow deflection angle along the sonic line

$$\Delta\theta^* = \theta_B^* - \theta_A^* \quad (18)$$

is divided in a number of equal intervals (ref. 7). Values of  $x^*$ ,  $y^*$ ,  $\phi^*$ , and  $\psi^*$  are then interpolated at these points along the sonic line by using cubic spline functions. Characteristics integration is performed in a line-by-line marching fashion from sonic-line initial data toward the point C of the triangular mathematical domain of dependence of the full-potential equation in a rheograph plane (fig. 4).

Step 3. - The mathematical domain of dependence should always be larger (fig. 5) than the physical, supersonic, shock-free zone that we are recomputing. With a very poor choice of parameter P in equations (13) and (14) it could happen that the mathematical domain of dependence will be smaller than the physical supersonic zone. Such a case is signaled automatically as an error, and the further execution of the CAS22 code is terminated. Yet another consequence attributable to the same cause is the occurrence of limit lines (ref. 19) inside the ABC mathematical domain of dependence. If limit lines do not protrude inside the physical supersonic domain, they are of no concern and the results of the computations are physically acceptable (ref. 14). If the limit lines occur inside the supersonic flow domain, the entire calculation should be repeated with a different (usually smaller) value of the input parameter P.

Coordinates of the partially new shape of the airfoil in a cascade are determined from the condition that the stream function must have the value  $\psi_s = 0$  everywhere on the surface of the airfoil. The third step of the design

procedure searches through the entire triangle ABC for the pairs of points where  $\psi$  changes its sign. At these points  $\phi_s$  and  $\theta_s$  are interpolated, and the new airfoil surface coordinates  $x_s$  and  $y_s$  between the points A and B are found by integrating the following expressions:

$$dx_s = d\phi_s \frac{\cos \theta_s}{(\rho/\rho_*)_s} - d\psi_s \frac{\sin \theta_s}{(\rho/\rho_*)_s} \quad (19)$$

$$dy_s = d\phi_s \frac{\sin \theta_s}{(\rho/\rho_*)_s} + d\psi_s \frac{\cos \theta_s}{(\rho/\rho_*)_s} \quad (20)$$

### COMPUTER PROGRAM General Description

Computer program CAS22 was developed with the intention to create a single program (fig. 6) that can operate either as an analysis code or as a shock-free design code for airfoil cascade flows. The analysis portion of CAS22 represents a modified version of the CAS2D analysis code for transonic cascades (ref. 8). In the design section of CAS22, subroutines CHASON and INVERS represent modified versions of their counterparts in the shock-free design code for isolated airfoils developed by Sobieczky (ref. 14).

Computer program CAS22 consists (fig. 6) of the MAIN routine and subroutines. Subroutine MAIN reads the input data from unit 5 and generates x,y computational grid coordinates by calling subroutines CONMAP, SPLIF, INTPL, REMAP and XYINF. The grid (fig. 7) is generated very efficiently (refs. 8 and 20) by utilizing conformal mapping, elliptic polar coordinates, and nonorthogonal coordinate stretching and shearing transformations. CAS22 can generate a maximum of four consecutively refined grids. Subroutine CONMAP performs point-by-point conformal mapping from the physical x,y plane (fig. 7) into the X,Y computational rectangular domain (fig. 8). Subroutines SPLIF and INTPL represent simplified versions of the cubic spline-fitting and interpolation routines. Subroutine REMAP performs remapping from the X,Y computational rectangular domain back into the x,y plane. Subroutine XYINF modifies the positions of the grid points at upstream and downstream infinity and specifies x,y coordinates of imaginary grid points and periodic grid points.

Subroutine ANALYS performs an iterative line overrelaxation of the continuity equation in its conservative form (eq. (1)). ANALYS actually generates coefficients of the three-diagonal correction matrix  $[C_{ij}]$

$$[C_{ij}] \{\phi_j\} = \{R_j\} + \{V_j\} \quad (21)$$

obtained from an artificially time-dependent form

$$\rho \left( \left( 1 - M_\infty^2 \right) \phi_{,ss} - \phi_{,nn} + 2C_s \phi_{,st} + 2C_n \phi_{,nt} + \epsilon \phi_{,t} \right) = 0 \quad (22)$$

(refs. 8, 13, and 20) of the full-potential equation (2). The vector of residuals  $\{R_j\}$  is evaluated by applying a finite area technique (refs. 20, and 21) to equation (1). ANALYS uses isentropic relations only (eqs. (4) and (5)) and

captures all possible existing shocks (isentropic discontinuities) by performing a type-dependent, rotated finite differencing (refs. 8, 13, 20, and 21) on the following artificially time-dependent form of equation (22):

$$\rho(1 - M_*^2)\phi_{,ss}^H - \rho(1 - M_*^2)\phi_{,ss}^E + \rho\left(\left(\nabla^2\phi^E - M_*^2\phi_{,ss}^E\right) + 2c_s\phi_{,st} + 2c_n\phi_{,nt} + \epsilon\phi_{,t}\right) = 0 \quad (23)$$

Here H designates upstream differencing and E designates central differencing to be performed on the  $\phi_{,xx}$ ,  $\phi_{,yy}$ , and  $\phi_{,xy}$  derivatives constituting  $\phi_{,ss}$  or  $\nabla^2\phi$  (refs. 8 and 20). The artificial viscosity vector  $\{V_j\}$  represents the difference between upstream and centrally differenced  $\phi_{,ss}$  derivatives in the first part of equation (23).

As already mentioned, ANALYS captures isentropic shocks that differ in their strength and position from the Rankine-Hugoniot shocks. For the purpose of gaining a user's confidence in the capabilities of the CAS22 code to solve a full potential equation, it is advisable to compare the results of CAS22 with the exact results obtained iteratively from mass conservation (ref. 16)

$$M_{*a} M_{*b} = M_{*a}^2 \frac{\rho_a}{\rho_b} \quad (24)$$

A comparison of exact values for the isentropic and Rankine-Hugoniot jumps in Mach numbers across a normal shock is shown in figure 9.

Boundary and periodicity boundary conditions are applied explicitly in subroutine ANALYS and in subroutine BOUND. When CAS22 is to operate as a shock-free design code, it will automatically switch to subroutine XDES (fig. 6) instead of ANALYS. Routine XDES uses isentropic-gas relation at all the grid points where the flow is subsonic. At the points where  $M_* > 1$ , subroutine XDES uses the fictitious-gas relations (eqs. (13) and (14)) for fluid density and the speed of sound. In such a way the full-potential equation is prevented from ever becoming locally hyperbolic, and the shock-free supersonic zones are created. Subroutine XDES thus represents step 1 of the shock-free design process described earlier. Step 2 is embodied in subroutine BUBBLE, which searches for the existence of shock free supersonic zones and determines the values of  $x^*$ ,  $y^*$ ,  $\phi^*$ ,  $\psi^*$ , and  $\theta^*$  along their respective sonic lines. BUBBLE can perform this task on an arbitrary number of supersonic zones on a one-by-one basis starting at the trailing edge and moving clockwise around the airfoil. BUBBLE can treat even supersonic geometric leading edges, but it cannot treat choked shock-free flows. Step 3 of the design procedure involves subroutines CHASON and INVERS. CHASON performs characteristics integration of  $x$ ,  $y$ ,  $\phi$ , and  $\psi$  inside the triangle ABC (figs. 4 and 5) in the rheograph plane by using isentropic relations. INVERS iteratively inverts the Prandtl-Meyer function (ref. 7).

After the integration is over, CHASON searches for the values of  $x_s$  and  $y_s$  where  $\psi = 0$  inside ABC. These are the new coordinates of the shock-free airfoil in the interval between points A and B (fig. 5). CHASON also searches for the existence of the limit lines inside the supersonic zones. After step 3 of the fictitious-gas, shock-free design procedure is finished, the CAS22 program proceeds with the closing subroutine CPMACH, or it automatically switches to its analysis mode. This switching capability is regulated by a single input parameter (explained

later). CPMACH calculates and prints surface Mach number, critical local Mach number, surface density, and the coefficient of pressure and plots (with the line printer) a rough plot of the  $C_p$ -distribution on the surface of the airfoil in a cascade. If the iterative calculation process is to be repeated on one or more additionally refined grids, subroutine MESH is called instead of CPMACH. MESH doubles the number of grid cells in each computational direction X and Y. MESH then interpolates values of the potential function obtained on the previous coarser grid onto the new grid by calling SPLIF and INTPL. In such a way an improved initial guess is created for the potential field calculation on the new refined grid.

## INPUT

The input data for CAS22 are identical to the input for the CAS2D program (ref. 8). The only difference is the addition of one computer card between cards 6 and 7 in CAS2D input. This inserted card contains the following three additional input parameters:

- TITR4 maximum number of iterations to be performed on the final (fourth) grid by routine ANALYS or by routine XDES. In the CAS2D program this value was predetermined to be one half of TITR3.
- SUPCEL number of equal angle increments to be generated along each sonic line between points A and B (figs. 4 and 5) before the characteristics integration is performed by CHASON. The maximum allowed value for SUPCEL is 299, although it is quite satisfactory to work with SUPCEL = 100.
- FCTGAS fictitious-gas constant P to be used in equations (13) and (14). It is the most important input parameter in the CAS22 program because it also determines the operating mode of the program according to the following rules:
- FCTGAS > 0.11: CAS22 works as a design code  
 FCTGAS > 0. but < 0.1: CAS22 works as an analysis code  
 FCTGAS < 0.: CAS22 works as a design code followed automatically by the analysis mode in order to confirm that the newly obtained airfoil shape in a cascade is truly shock free. Actually the relation between FCTGAS and the constant P in equations (13) and (14) is

$$P = |FCTGAS|$$

The user of CAS22 should be aware that he can to a certain degree influence the shape of the resulting  $C_p$ -distribution. Very low (absolute) values of FCTGAS will barely smear out the original shocks. Very high (absolute) values of FCTGAS will produce a highly "peaky"  $C_p$ -distribution (ref. 15) and will increase the chance of a limit-line occurrence inside the supersonic flow domain. Generally acceptable values (absolute) of FCTGAS are

$$5. < |FCTGAS| < 500.$$

This new card in the input of CAS22 has the same format (2x, 3 (7x, E12.5) as the original first few cards in the input of CAS2D (ref. 8). Examples of several inputs for the CAS22 program are shown in figures 11, 17, 20, 27, 32, 33, 34, 39.

## OUTPUT

The output from CAS22 is almost identical with the output from the CAS2D program (ref. 8). Again, the present version of CAS22 does not have any need for tapes

although additional command for writing the results on a unit 14 can be easily incorporated. The difference between the output from CAS2D and CAS22 is that CAS22 prints surface pressure, density, Mach number, etc., distribution only (ref. 8) after the solution has converged or the the maximum number of iterations has been reached on the final grid. CAS22 does not print out the Mach number chart (ref. 8), but it finishes the output with a rough printer-plot of the airfoil surface pressure coefficient calculated from the equation

$$C_p = \frac{p - p_{\infty}}{\frac{1}{2} \rho_{\infty} q_{\infty}^2} \quad (25)$$

with  $p_{\infty} = 1$ ,  $\rho_{\infty} = 1$  and  $q_{\infty} = 1$ .

#### ASSUMPTIONS, LIMITATIONS, AND APPLICABILITY OF COMPUTER PROGRAM CAS22

Computer program CAS22 is directly applicable for the analysis of transonic, steady, inviscid, and irrotational flow through two-dimensional static cascades of given airfoils. CAS22 is also directly applicable for the design (determination of coordinates of the points defining an airfoil shape) of shock-free airfoil shapes for transonic, steady, inviscid and irrotational cascade flow. It should be remembered that in both of these applications the identical program CAS22 is used. Only the inputs to CAS22 in these two operation modes vary. The difference in the inputs is confined to a single input parameter.

In its analysis mode CAS22 can predict flow fields ranging in local speeds from incompressible through transonic, including the possible discontinuities (ref. 8) in the solution of the full-potential equation. These isentropic discontinuities do not represent physical shock waves because they do not satisfy Rankine-Hugoniot shock jump conditions (fig. 9). This suggests implicitly a basic assumption that all possible aerodynamic shocks must be weak (Mach number just ahead of the discontinuity should be  $Ma < 1.3$ ) so that the entropy (actually vorticity) generated by them is negligible. The following assumption is that the boundary layer does not separate. Users should be aware that CAS22 does not calculate the boundary layer displacement thickness, the shock-boundary layer interaction, or the trailing-edge viscous effects. A separate computer program should therefore be added to CAS22 in the future that takes into account these phenomena. Cascades of closely spaced, highly cambered, thick turbine blades cannot be handled by the present CAS22 (refs. 8 and 20) grid-generation technique.

On the other hand, CAS22 can be successfully used for the analysis and shockless design of isolated airfoils by giving the gap-chord input parameter a value of, say,  $PITCH = 30$ .

#### RESULTS

To demonstrate the capabilities of the CAS22 computer program in its design and flow analysis application, a series of numerical test cases (fig. 10) were conducted.

For the purpose of simplifying input data preparation, coordinates of input airfoils were generated by using an analytic expression

$$y = Ax + Bx^C + \sqrt{x(1-x)} (D + Ex + Fx(1-x)) \quad (26)$$

developed by Sobieczky (ref. 16 and DFVLR internal report, "Design Examples for Super-Critical Cascades", by H. Sobieczky and D. S. Dulikravich, to be published). Here A, B, C, D, E, and F are appropriate constants affecting the airfoil thickness, the curvature of the leading and trailing edges, and the mean camber line. Numerical flow calculations for each test case were performed on four successively refined, boundary-conforming, geometrically periodic grids of an O type.

After 200 iteration cycles were performed on the first grid, the potential field was interpolated on the second grid, on which an additional 200 iteration sweeps were performed. The potential function was then interpolated on the third grid, where 100 iterations were performed. Finally this potential field was interpolated on the fourth grid, where it served as an initial guess for the concluding 100 iterations (TIIR4 = 100.), after which the potential field was considered converged for the engineering applications. The grid sequence used in both the analysis and design modes was the following: first grid, 24 x 6 grid cells, second grid, 48 x 12 grid cells, third grid, 96 x 24 grid cells, and fourth grid, 192 x 48 grid cells. The number of refined computational grid cells along each sonic line (fig. 5) was SUPCEL = 98. Wake and boundary layer displacement thickness were not taken into account. The specific heat ratio used in the isentropic relations was  $\gamma = 1.4$ . All calculations were performed on an IBM 3033 computer.

Test case 1 is an airfoil cascade with the following specifications: stagger angle  $\beta$ ,  $-50^\circ$ ; free-stream angle at upstream infinity  $\alpha_1$ ,  $65^\circ$ ; free-stream angle at downstream infinity  $\alpha_2$ ,  $42^\circ$ ; Mach number at upstream infinity  $M_1$ , 0.80; gap-chord ratio  $g/c$ , 0.8.

The entire input for test case 1 is shown in figure 11. An analysis mode of the CAS22 program with FCTGAS = 0. shows (figs. 12 and 13) that this highly staggered cascade flow has a single supersonic zone terminated by a strong shock. A design mode of CAS22 (with FCTGAS = 25.) "shaves off" this original airfoil cascade and creates a new shock-free (figs. 14 and 15) cascade flow field. It should be pointed out again that the actual change in the airfoil shape is performed only along the section wetted by the supersonic flow. From figure 16 it can be concluded that the changes are infinitesimally small and reflect the extreme sensitivity of the transonic cascade flow to any changes in global flow conditions or in the cascade airfoil shape. Figure 16 also shows that the entire flow field is shock free.

For the industrial application of shock-free cascades it is very important to know how they perform at off-design conditions. To provide an illustrative answer to this question, coordinates of the newly obtained shock-free airfoil were substituted in the input data (fig. 17) set with an off-design, free-stream Mach number at upstream infinity  $M_1 = 0.78$ . With this input (fig. 17) an analysis mode (FCTGAS = 0.) of CAS22 shows that the shock-free cascade reverts to a shocked cascade at off-design conditions. The question is now; Is this shock stronger or weaker than the shock that exists in the original cascade at the same off-design conditions? The answer is presented in figures 18 and 19. It is apparent that the shock-free airfoil cascade performs better than the original shocked cascade even at off-design conditions. The shock-free cascades will have shocks at off-design conditions, but these shocks will be weaker and the losses due to shock - boundary layer separation and shock wave drop will be less. In addition, their supersonic zones will be flatter, thus delaying the occurrence of choking flow conditions.

Test case 2 (fig. 10) has the purpose of showing that CAS22 is capable of converting relatively thick airfoil shapes into shock-free shapes. Input data for test case 2 are shown in figure 20. With this input CAS22 reveals (figs. 21 and 22) that the original cascade has two supersonic zones terminated by strong shocks.

This cascade was then converted into a shock-free cascade (figs. 23 and 24) that has a remarkably thin and elongated supersonic zone on the suction surface (fig. 25). To show the improvement in aerodynamic efficiency of the cascade over a range of free-stream inlet Mach numbers, this new shock-free cascade was analysed (fig. 26) at a number of off-design Mach numbers. One of the input data sets for these analyses is shown in figure 27. For weak shocks the shock wave drag losses are approximately proportional to the third power of the drop in Mach number  $\Delta M$  across the shock. It is clear from figure 26 that the shock free cascade designed by using the fictitious-gas concept offers better performance over a range of inlet Mach numbers although the shock-free design was performed only for a single value of  $M_1 = 0.72$ .

Test case 3 has the purpose of showing that CAS22 is capable of both analysis (figs. 28 and 29) and a fictitious gas, shock-free redesign (figs. 30 and 31) of high-solidity ( $g/c = 0.6666$ ), moderate-stagger ( $\beta = -25^\circ$ ) airfoil cascades. Note that the original cascade has a supersonic zone starting very close to the leading edge. Input data for the redesign of the original cascade in test case 3 are shown in figure 32. Input data for the analysis of the newly obtained shock-free cascade in test case 3 are shown in figure 33. The value of FCTGAS used in this test case (fig. 10) was somewhat lower, because the higher values would cause very peaky surface pressure distribution and possibly limit lines inside the supersonic part of the flow field.

Test case 4 has the purpose of showing in a simple way the capability of CAS22 to unchoke already choked, shocked cascade flows and to make the unchoked flow fields entirely shock free. A nonstaggered cascade of NASA 0018 airfoils was analysed with  $M_1 = 0.582$ . The flow is obviously choked (figs. 34 and 35) because even one-dimensional analysis predicts (ref. 22) that this flow will choke if  $M_1 > 0.577$ . A design mode of CAS22 with  $P = 500$ . (eqs. (13) and (14)) converted this flow field into the shock-free unchoked cascade flow shown in figures 36 to 38. Coordinates of the new shock-free NACA 0018 airfoil cascade are shown in figure 39.

The computer time required for each test run varied between 290 CPU seconds and 330 CPU seconds on an IBM 3033 computer. Total core memory required was on the average 500K.

#### CONCLUSIONS, SUGGESTIONS, AND PERSPECTIVES

The fictitious-gas concept of Sobieczky was successfully applied in a design procedure for shock-free, two-dimensional airfoil cascades. Computer programs like CAS22 can be relatively simply developed from the existing full-potential analysis codes for compressible (not necessarily supersonic) flow fields. CAS22 represents a fast computer program ready for use by aerodynamicists with practically no knowledge of numerical methods and computer programming. A very concise and simple to understand input format is designed specifically for such users. The entire code is well documented by the comment cards, and possible changes or modifications can be easily added or inserted. In its present version CAS22 does not have a need for any tapes or disks. The entire output, containing coordinates of the new shock-free airfoil surface and the corresponding values of coefficient of pressure, density, Mach number, and critical Mach number, is printed on paper. If one desires to save them permanently for the purpose of a computer graphics display, WRITE(14) cards in the routines MAIN and BUBBLE should be reactivated. Each of them has an adjacent self-explanatory comment card. It should be clearly pointed out that the locations

of airfoil leading-edge and trailing-edge stagnation points are not fixed in CAS22 but will change during the course of iteration. They will finally be forced to settle at the locations on the airfoil surface that are compatible with the input data parameters,  $\alpha_1$ ,  $\alpha_2$ ,  $M_1$ ,  $\beta$ , and  $g/c$ . For closely spaced blades at transonic speeds, the flow field at the trailing edge is mostly influenced by the value of  $\alpha_2$ . Nonrealistic values of any of these input parameters and especially of  $\alpha_2$  will force the trailing-edge stagnation point to move away from the geometric trailing-edge location. This will result in excessively high supersonic Mach numbers at the trailing edge as the flow is forced to go around it. As a result the CAS22 iterative procedure will quickly diverge and the program execution will terminate. The iterative calculation performed by CAS22 sometimes terminates if the user attempts to calculate choked flows, although it does not always happen. Termination or simply oscillatory iteration can also occur if one tries to redesign a shocked cascade with the Mach number just ahead of the shock higher than approximately  $M_a = 1.35$ .

If the user is not satisfied with the resulting shock-free surface pressure distribution, he can try two things: either repeat the run with a different value of the input parameter FCTGAS, or repeat the run with a slightly changed input airfoil shape. The second option gives a user an almost endless possibility to generate significantly different shock-free surface pressure distributions by simply adding shallow "bumps" to the original airfoil surface so that CAS22 will have more freedom to perform its "shaving" procedure.

CAS22 does not take into account boundary layer displacement thickness although it can include the global wake blockage effect (ref. 8) via the input parameter AR. Any shock free cascade flow designed by CAS22 will be theoretically shock free only for a single set of input parameters. If any one of these parameters is changed, shocks will occur. Use of CAS22 in connection with an optimization program should generate airfoil shapes that offer the best aerodynamic efficiency (weakest shocks) over a specified range of, say, inlet Mach numbers.

Use of existing analysis codes to clarify that the shock-free flow field is actually shock free as predicted by CAS22 can give slightly varying results depending on the accuracy of the numerical scheme used (ref. 23) and the grid resolution used in the particular analysis code. Figure 40 shows a comparison (ref. 16) between the results obtained from a design mode of CAS22 and the results of analysis obtained by the analysis mode of CAS22 and by an Euler equation solver (provided by Dr. David Ives of Pratt and Whitney Aircraft Company aerodynamics research staff) developed by Ni (ref. 24). CAS22 analysis version gives slightly sharper recompression due to the first order artificial viscosity used in ANALYS.

Extension of the applications of the fictitious-gas technique to quasi-three-dimensional stator shock-free blade design was recently accomplished (ref. 25). The final goal is a fully three-dimensional, shock-free rotor blade and hub design capability.

#### REFERENCES

1. Garabedian, P. R., "Partial Differential Equations", John Wiley and Sons, New York, 1964.
2. Swenson, E. V., "Geometry of the Complex Characteristics in Transonic Flow", Communications on Pure and Applied Mathematics, vol. XXI, 175-185, (1968).
3. Korn, D., "Numerical Design of Transonic Cascades", Courant Institute of Mathematical Sciences, ERDA Research and Development Report C00-3077-72, January 1975.



4. Ives, D. C. and Liutermoza, J. F., "Second Order Accurate Calculation of Transonic Flow Over Turbomachinery Cascades", AIAA Paper No. 78-1148, presented at AIAA 11th Fluid and Plasma Dynamics Conference, July 10-12, 1978, Seattle, Washington.
5. Sobieczky, H., "Entwurf eines transsonischen Kompressorengitters", DFVLR IB 251-77 A 22, July 28, 1977.
6. Schmidt, E., "Computation of Supercritical Compressor and Turbine Cascades with a Design Method for Transonic Flows", ASME Paper No. 79-GT-80, 1979.
7. Sobieczky, H., "Transonic Fluid Dynamics - Lecture Notes," The University of Arizona, TFD 77-01, Oct. 1977.
8. Dulikravich, D. S., "CAS2D - Fortran Program for Nonrotating Blade-to-Blade, Steady, Potential Transonic Cascade Flows," NASA TP-1705, 1980.
9. Volpe, G. and Melnik, R. E., "The Role of Constraints in the Inverse Design Problem for Transonic Airfoils", AIAA Paper No. 81-1233 presented at AIAA 14th Fluid and Plasma Dynamics Meeting, June 23-25, 1981, Palo Alto, California.
10. Shapiro, A. H., "The Dynamics and Thermodynamics of Compressible Fluid Flow-Volume I", The Ronald Press Company, New York, 1953, p. 470-473.
11. Sobieczky, H., "Related Analytical, Analog and Numerical Methods in Transonic Airfoil Design", AIAA paper no. 79-1556, presented at AIAA 12th Fluid and Plasma Dynamics Conference, July 23-25, 1979, Williamsburg, Virginia.
12. Sobieczky, H., Fung, K-Y., Yu, N. and Seebass, R., "A New Method for Designing Shock-free Transonic Configurations," AIAA Journal, Vol. 17, no. 7, July 1979, pp. 722-729.
13. Jameson, A., "Transonic Flow Calculations," in Computational Fluid Dynamics, Vol. 1, Von Karman Institute, VKI-LS-87-VOL-1, 1976, pp. 1.1-5.84.
14. Sobieczky, H., "Rheograph Transformation and Continuation Methods," in Mathematical Methods in Fluid Mechanics, Von Karman Institute for Fluid Dynamics, VKI-LS-1980-4, Feb. 1980.
15. Sobieczky, H., "Design of Advanced Technology Transonic Airfoils and Wings," Subsonic/Transonic Configuration Aerodynamics, AGARD Fluid Dynamics Panel Symposium, AGARD CP-285, 1980.
16. Dulikravich, D. S. and Sobieczky, H., "Shockless Design and Analysis of Transonic Blade Shapes," AIAA Paper No. 81-1237 or NASA TM 82611 presented at the 14th AIAA Fluid Plasma Dynamics Conference, Palo Alto, California, June 23-25, 1981.
17. Fung, K-Y., Sobieczky H. and Seebass R., "Numerical Aspects of the Design of Shock-Free Wings", AIAA Paper No. 79-1557, presented at the AIAA 12th Fluid and Plasma Dynamics Conference, July 23-25, 1979, Williamsburg, Virginia.
18. Yu, N. J., "An Efficient Transonic Shock-Free Redesign Procedure Using a Fictitious Gas Method," AIAA Paper No. 79-0075.
19. Tsien, H. S., "Limiting Line in Mixed Subsonic and Supersonic Flow of a Compressible Fluid", NACA TN 961 (1944).
20. Dulikravich, D. S., "Numerical Calculation of Inviscid Transonic Flow Through Rotors and Fans," Ph.D. Thesis, Cornell University, January 1979. (Available through University Microfilms International, 300 N. Zeeb Road, Ann Arbor, Michigan 48106.)
21. Jameson, A., and Caughey, D., "A Finite Volume Scheme for Transonic Potential Flow Calculations," AIAA 3rd Computational Fluid Dynamics Conference, 1977, Paper 77-635, pp. 35-54.
22. Equations, Tables and Charts for Compressible Flow", NACA TR-1135, 1953.

23. Caughey, D. and Jameson, A., "Basic Advances in the Finite-Volume Method for Transonic Potential Flow Calculations", Presented at the Symposium on Numerical and Physical Aspects of Aerodynamic Flows, Long Beach, California, January 19-21, 1981.
24. Ni, R. H., "A Multiple Grid Scheme for Solving the Euler Equations", AIAA paper no. 81-1025, presented at 5th AIAA Computational Fluid Dynamics Conference, Palo Alto, California, June 22-23, 1981.
25. Beauchamp, P., "A Numerical Tool for the Design of Shock-Free Transonic Cascades", M. Sc. Thesis, Aerospace Engineering Department, University of Arizona, Tucson, AZ, June 1981

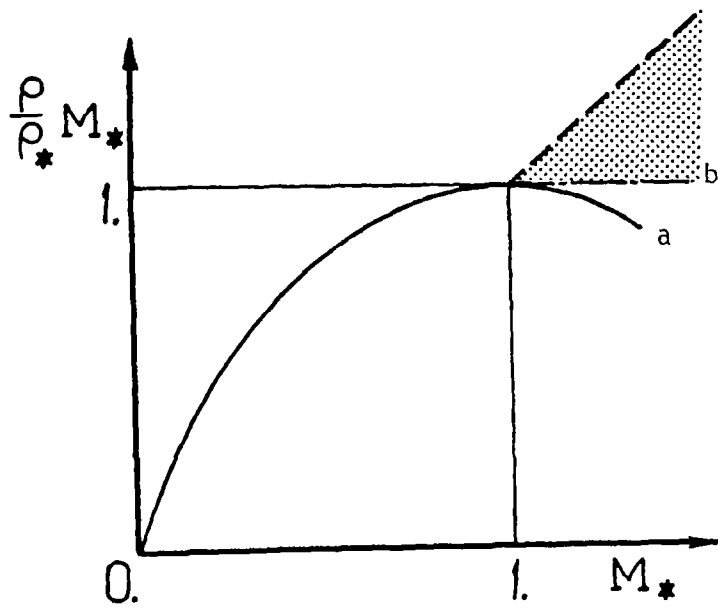


Figure 1. - Relation between isentropic (a) parabolic (b) and fictitious mass flow domain

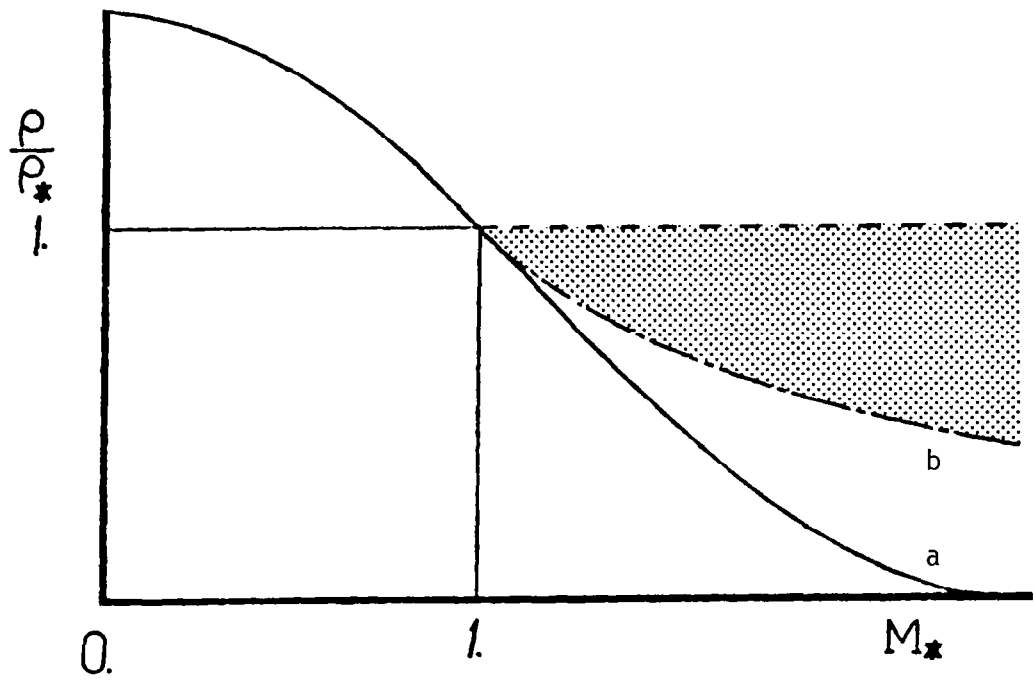


Figure 2. - Relation between isentropic (a), parabolic (b) and fictitious density domain

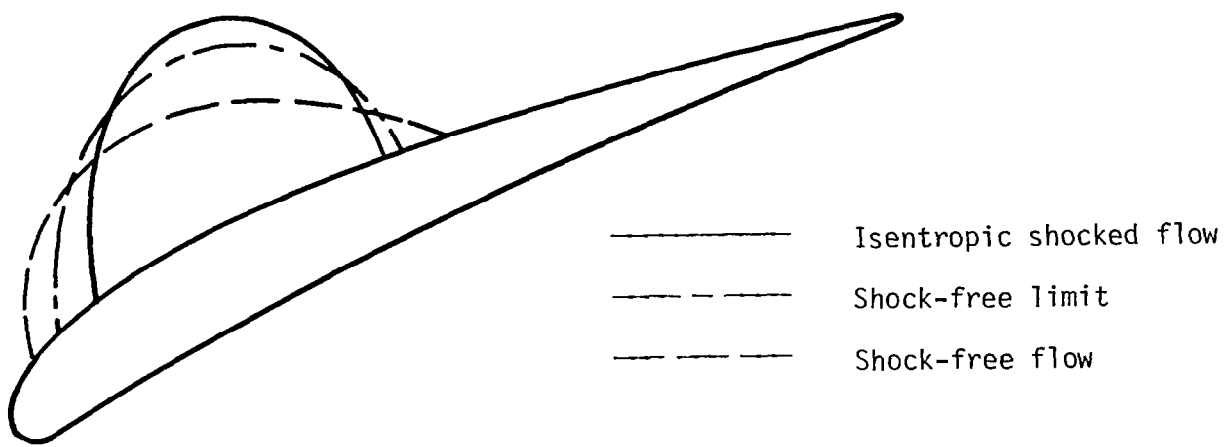


Figure 3. - Example of the sonic line shapes compatible with the isentropic shocked flow, parabolic shock-free limit, and a shock-free flow obtained by using fictitious-gas relations

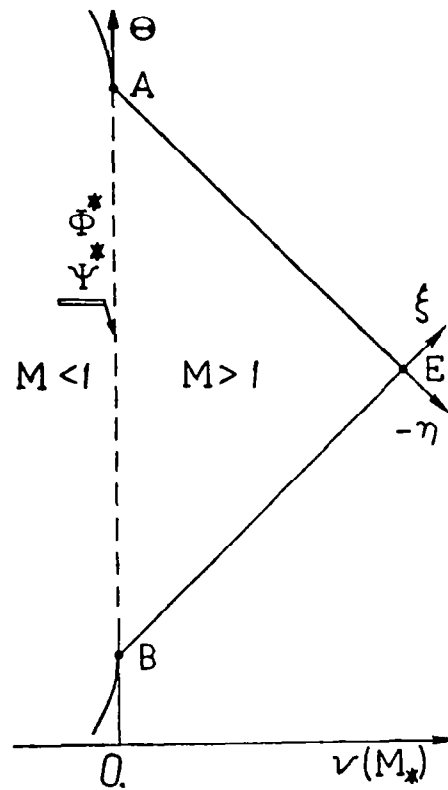
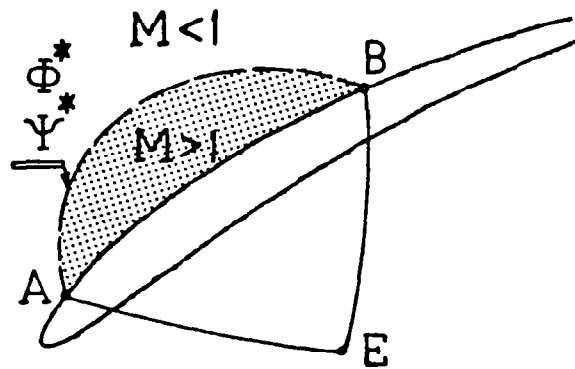


Figure 4. - Domains of dependence of full-potential equation in physical  $(x, y)$  and rheograph  $(\theta, \nu)$  planes

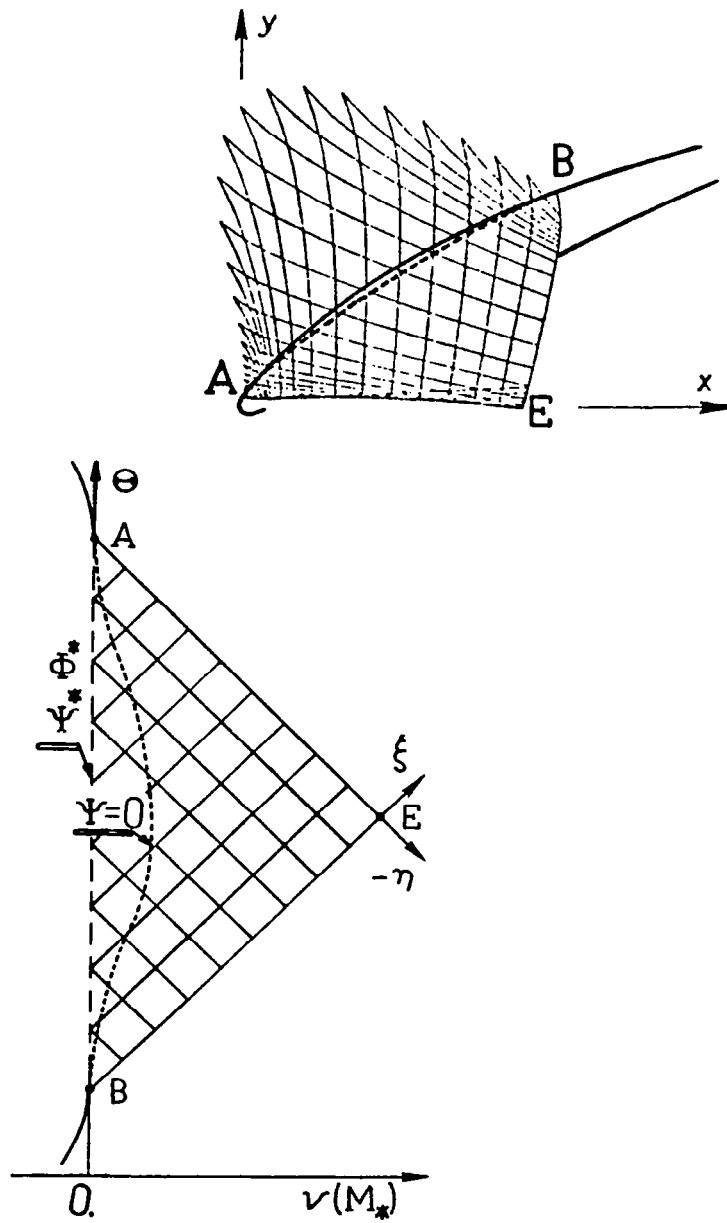


Figure 5. - Characteristic grid in physical and rheograph plane with shape of new (shock free) surface

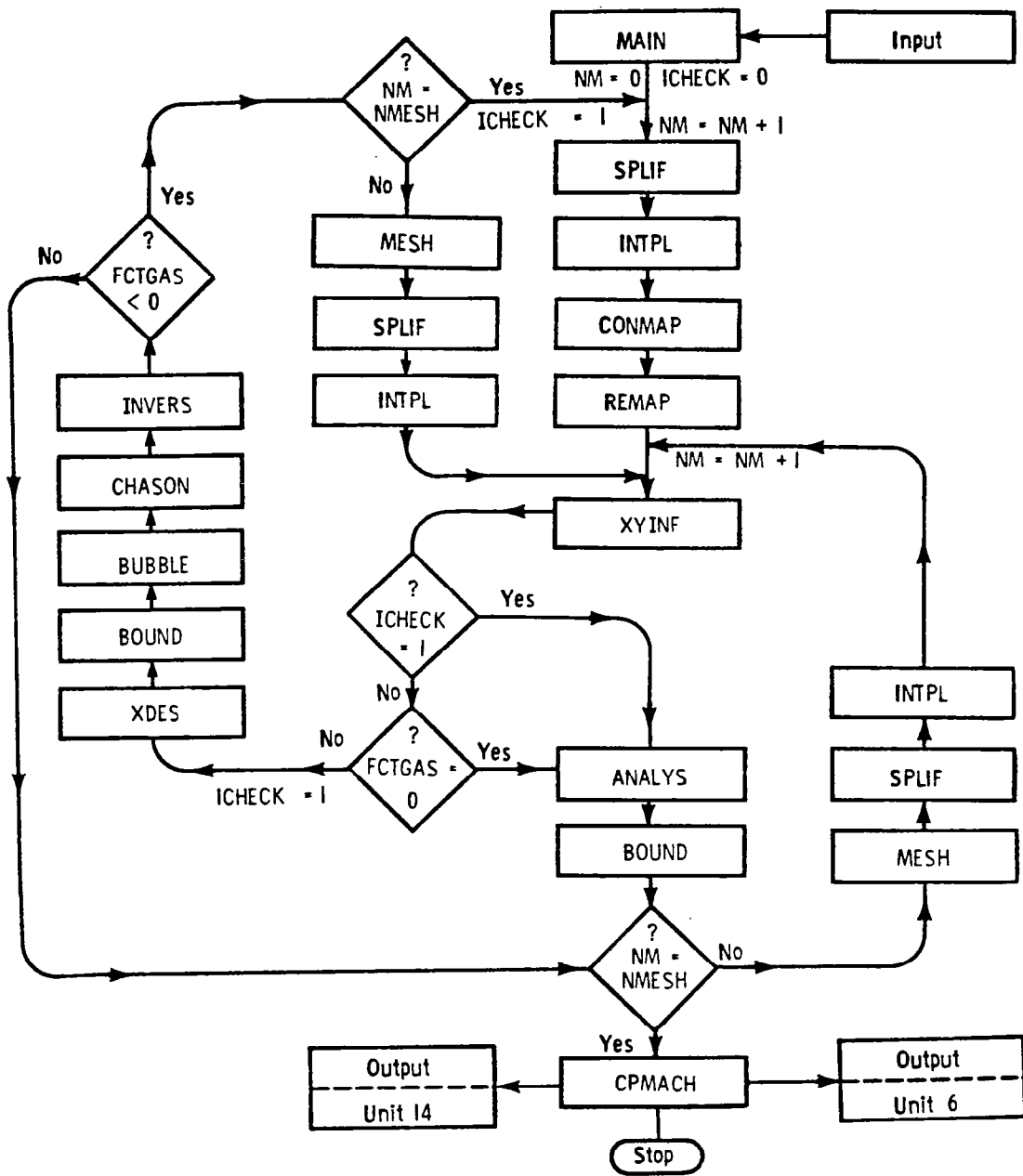


Figure 6. - Global flow chart of CAS22 program



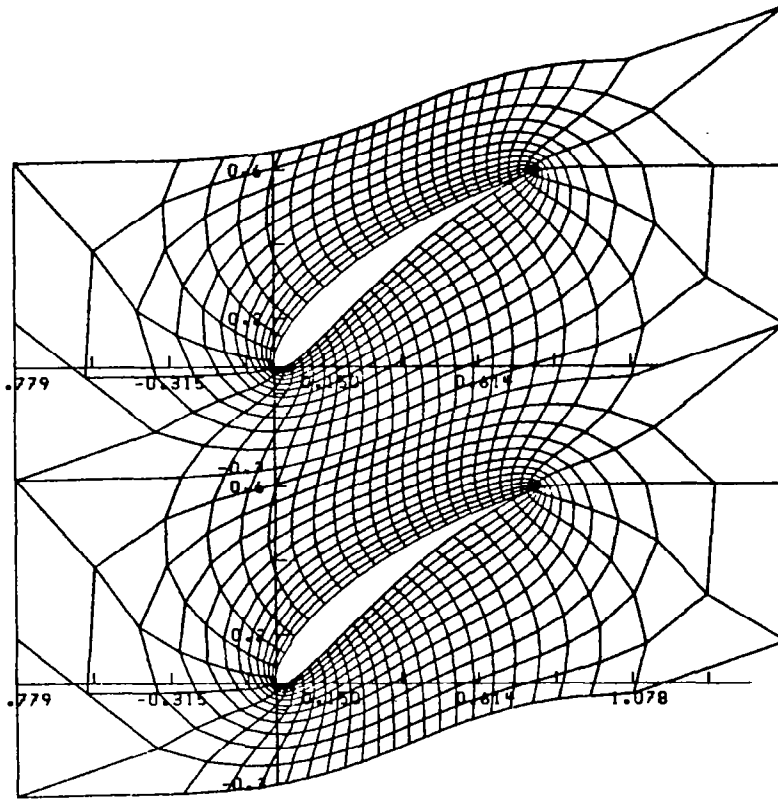


Figure 7. - Computational grid in physical (x,y) plane

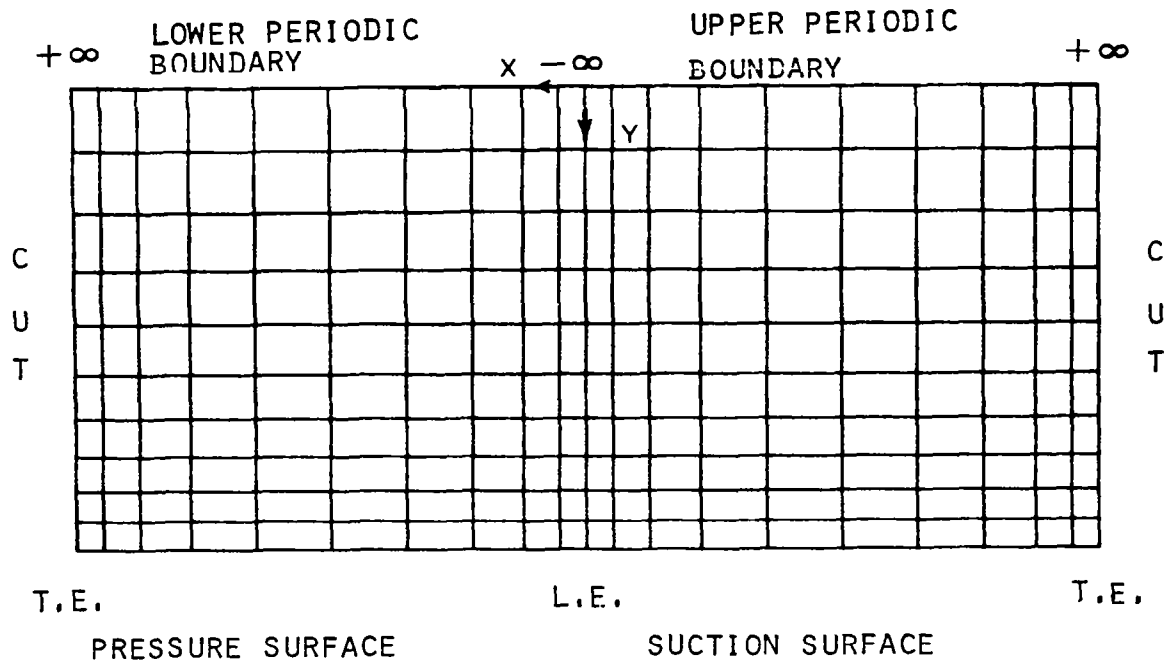


Figure 8. - Periodic flow field in computational (X,Y) plane

$M_a$	$M_a^*$	$M_b$	$M_b^*$	$\bar{M}_b$
1.00601	1.00500	0.99401	0.99500	0.99502
1.01204	1.01000	0.98804	0.99001	0.99010
1.01808	1.01500	0.98210	0.98502	0.98522
1.02415	1.02000	0.97617	0.98003	0.98039
1.03023	1.02500	0.97027	0.97504	0.97561
1.03633	1.03000	0.96439	0.97006	0.97087
1.04245	1.03500	0.95853	0.96508	0.96618
1.04859	1.04000	0.95269	0.96011	0.96154
1.05475	1.04500	0.94687	0.95514	0.95694
1.06093	1.05000	0.94107	0.95017	0.95238
1.06713	1.05500	0.93529	0.94520	0.94787
1.07335	1.06000	0.92952	0.94024	0.94340
1.07959	1.06500	0.92378	0.93528	0.93897
1.08585	1.07000	0.91806	0.93033	0.93458
1.09213	1.07500	0.91236	0.92538	0.93023
1.09843	1.08000	0.90668	0.92043	0.92593
1.10476	1.08500	0.90101	0.91548	0.92166
1.11110	1.09000	0.89537	0.91054	0.91743
1.11747	1.09500	0.88974	0.90560	0.91324
1.12385	1.10000	0.88413	0.90067	0.90909
1.13026	1.10500	0.87854	0.89574	0.90498
1.13670	1.11000	0.87297	0.89081	0.90090
1.14315	1.11500	0.86741	0.88589	0.89686
1.14963	1.12000	0.86188	0.88096	0.89286
1.15613	1.12500	0.85636	0.87605	0.88889
1.16265	1.13000	0.85086	0.87113	0.88496
1.16920	1.13500	0.84538	0.86622	0.88106
1.17577	1.14000	0.83991	0.86132	0.87719
1.18236	1.14500	0.83446	0.85641	0.87336
1.18898	1.15000	0.82903	0.85151	0.86957
1.19563	1.15500	0.82361	0.84662	0.86580
1.20229	1.16000	0.81821	0.84173	0.86207
1.20899	1.16500	0.81283	0.83684	0.85837
1.21571	1.17000	0.80747	0.83195	0.85470
1.22245	1.17500	0.80212	0.82707	0.85106
1.22922	1.18000	0.79678	0.82219	0.84746
1.23602	1.18500	0.79147	0.81732	0.84388
1.24284	1.19000	0.78617	0.81245	0.84034
1.24969	1.19500	0.78088	0.80759	0.83682
1.25656	1.20000	0.77561	0.80272	0.83333
1.26346	1.20500	0.77036	0.79787	0.82988
1.27039	1.21000	0.76512	0.79301	0.82645
1.27735	1.21500	0.75990	0.78816	0.82305
1.28434	1.22000	0.75469	0.78331	0.81967
1.29135	1.22500	0.74950	0.77847	0.81633
1.29840	1.23000	0.74433	0.77363	0.81301
1.30547	1.23500	0.73917	0.76880	0.80972
1.31257	1.24000	0.73402	0.76397	0.80645
1.31970	1.24500	0.72889	0.75914	0.80321
1.32686	1.25000	0.72377	0.75432	0.80000
1.33405	1.25500	0.71867	0.74950	0.79681
1.34128	1.26000	0.71358	0.74469	0.79365
1.34853	1.26500	0.70851	0.73988	0.79051
1.35581	1.27000	0.70345	0.73508	0.78740
1.36313	1.27500	0.69841	0.73028	0.78431
1.37048	1.28000	0.69338	0.72548	0.78125
1.37786	1.28500	0.68837	0.72069	0.77821
1.38527	1.29000	0.68337	0.71591	0.77519
1.39272	1.29500	0.67838	0.71112	0.77220
1.40020	1.30000	0.67341	0.70635	0.76923
1.40771	1.30500	0.66845	0.70157	0.76628
1.41526	1.31000	0.66351	0.69681	0.76336
1.42284	1.31500	0.65858	0.69204	0.76046
1.43046	1.32000	0.65366	0.68728	0.75758
1.43812	1.32500	0.64876	0.68253	0.75472
1.44581	1.33000	0.64387	0.67778	0.75188
1.45353	1.33500	0.63899	0.67304	0.74906
1.46129	1.34000	0.63413	0.66830	0.74627
1.46909	1.34500	0.62928	0.66357	0.74349
1.47693	1.35000	0.62445	0.65884	0.74074
1.48481	1.35500	0.61963	0.65412	0.73801
1.49272	1.36000	0.61482	0.64940	0.73529
1.50068	1.36500	0.61003	0.64469	0.73260
1.50867	1.37000	0.60525	0.63998	0.72993
1.51670	1.37500	0.60048	0.63528	0.72727
1.52477	1.38000	0.59572	0.63059	0.72464
1.53289	1.38500	0.59098	0.62590	0.72202
1.54104	1.39000	0.58626	0.62121	0.71942
1.54924	1.39500	0.58154	0.61654	0.71685

Figure 9. - Rankine-Hugoniot ( $\bar{M}_b$ ) and isentropic ( $M_b$ ,  $M_b^*$ ) shock jump relations

TEST CASE	ANALYSIS AND DESIGN INPUT PARAMETERS						OFF-DESIGN
	M <sub>1</sub> (FMACH)	β ° (TWIST)	α <sub>1</sub> ° (ALPHA1)	α <sub>2</sub> ° (ALPHA2)	G / C (PITCH)	P (FTCGAS)	M <sub>1</sub> (FMACH)
1	0.80	-50.	65.	42.	0.8	25.	0.78
2	.72	-27.	37.	16.	1.	30.	.70 / .75
3	.75	-25.	45.5	13.5	.6666	20.	
4	.582	0	0	0	1.	500.	

Figure 10. - Test cases for CAS22 program

```

TEST CASE NO.1 : ORIGINAL CASCADE
XCELL = 0.240000D+02YCELL = 0.060000D+02PMESH = 4.000000D+00
ALPHA1= 0.650000D+02TWIST =-0.500000D+02ALPHA2= 0.420000D+02
PITCH = 0.800000D+00R01 = 0.00631D+00R02 = 0.00050D+00
FMACH = 0.800000D+00RLX = 1.750000D+00AR = 1.000000D+00
TITR1 = 2.000000D+02TITR2 = 2.000000D+02TITR3 = 1.000000D+02
TITR4 = 1.000000D+02SUPCEL= 0.980000D+02FCTGAS= 0.825000D+03
POINTS= 1.250000D+02GAMMA = 1.400000D+00CONVER= 1.000000D-09
1.000000 0.600000
0.997529 0.596776
0.994917 0.594916
0.992027 0.593151
0.988722 0.591313
0.984871 0.589312
0.980347 0.587081
0.975032 0.584568
0.968815 0.581725
0.961593 0.578509
0.953277 0.574880
0.943784 0.570798
0.933048 0.566222
0.921013 0.561113
0.907637 0.555429
0.892891 0.549129
0.876762 0.542170
0.859250 0.534510
0.840368 0.526106
0.820145 0.516917
0.796623 0.506905
0.775857 0.496035
0.751916 0.484279
0.726879 0.471614
0.700839 0.458028
0.673895 0.443516
0.646161 0.428090
0.617754 0.411773
0.588801 0.394601
0.559433 0.376630
0.529787 0.357927
0.500000 0.338579
0.470213 0.318687
0.440567 0.298364
0.411199 0.277740
0.382246 0.256951
0.353839 0.236144
0.326105 0.215471
0.299161 0.195086
0.273121 0.175141
0.248084 0.155784
0.224143 0.137157
0.201377 0.119390
0.179855 0.102599
0.159632 0.086885
0.140750 0.072332
0.123238 0.059002
0.107109 0.046938
0.092363 0.036161
0.078987 0.026671
0.066952 0.018447
0.056216 0.011450
0.046723 0.005619
0.038407 0.000881
0.031185 -0.002851
0.024968 -0.005673
0.019653 -0.007684
0.015129 -0.008977
0.011278 -0.009631
0.007973 -0.009680
0.005083 -0.009067
0.002471 -0.007432
0.000000 0.000000
0.002471 0.012353
0.005083 0.019155
0.007973 0.025456
0.011278 0.031874
0.015129 0.038714
0.019653 0.046164
0.024968 0.054354
0.031185 0.063370
0.038407 0.073266
0.046723 0.084071
0.056216 0.095790
0.066952 0.108406
0.078987 0.121888
0.092363 0.136186
0.107109 0.151237
0.123238 0.166967
0.140750 0.183294
0.159632 0.200128
0.179855 0.217374
0.201377 0.234935
0.224143 0.252716
0.248084 0.270619
0.273121 0.288552
0.299161 0.306426
0.326105 0.324157
0.353839 0.341667
0.382246 0.358882
0.411199 0.375738
0.440567 0.392175
0.470213 0.408137
0.500000 0.423579
0.529787 0.438458
0.559433 0.452736
0.588801 0.466383
0.617754 0.479372
0.646161 0.491680
0.673895 0.503290
0.700839 0.514191
0.726879 0.524372
0.751916 0.533832
0.775857 0.542572
0.798623 0.550597
0.820145 0.557917
0.840368 0.564549
0.859250 0.570512
0.876762 0.575828
0.892891 0.580527
0.907637 0.584639
0.921013 0.588197
0.933048 0.591240
0.943784 0.593806
0.953277 0.595935
0.961593 0.597670
0.968815 0.599052
0.975032 0.600124
0.980347 0.600924
0.984871 0.601490
0.988722 0.601853
0.992027 0.602032
0.994917 0.602021
0.997529 0.601738
1.000000 0.600000

```

Figure 11. - Test case 1 input data set (design mode) for original airfoil cascade

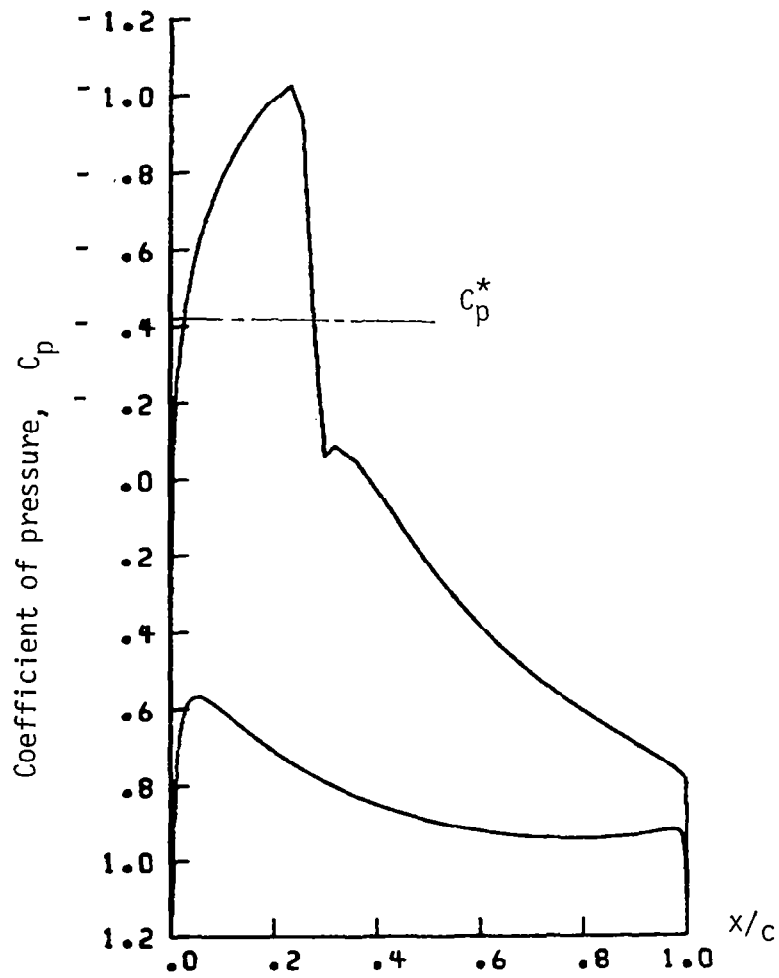


Figure 12. - Test case/coefficient-of-pressure distribution for original cascade

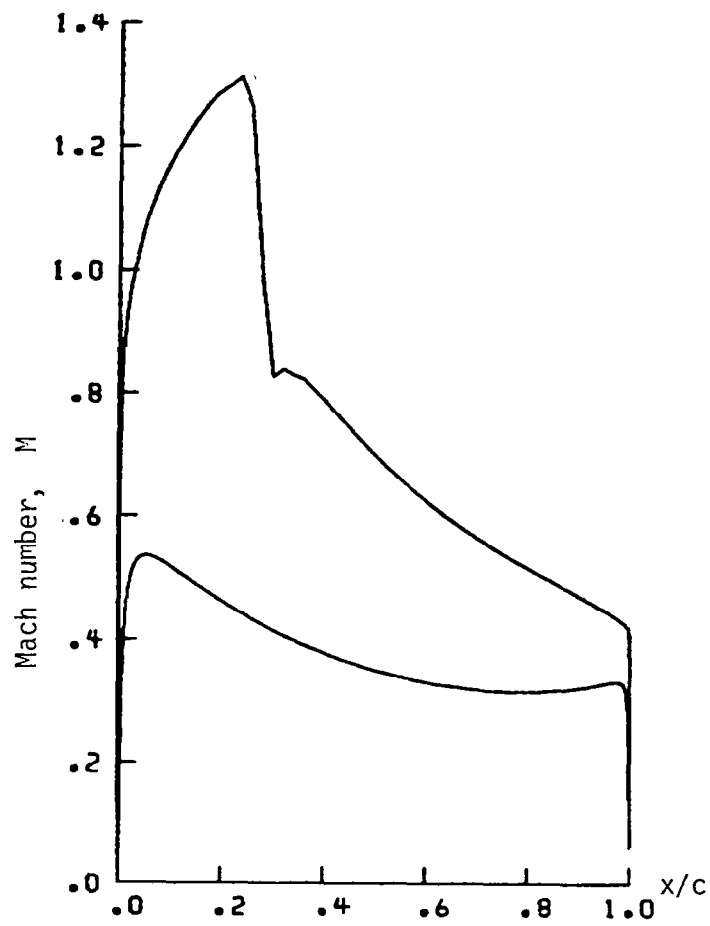


Figure 13. - Test case / Mach number distribution for original cascade

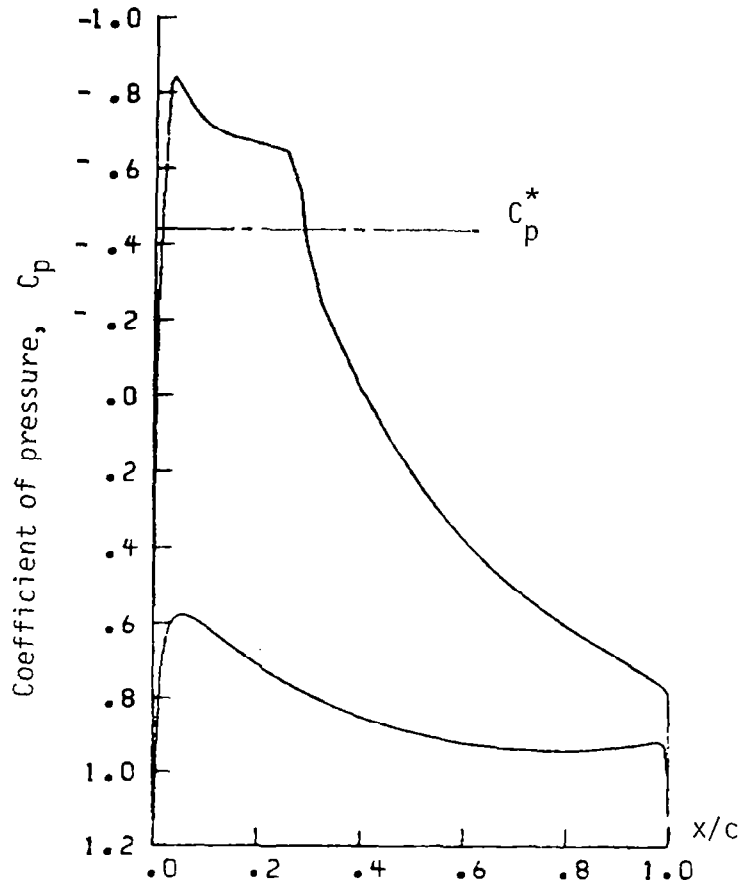


Figure 14.- Test case/coefficient-of-pressure distribution for designed shock-free cascade



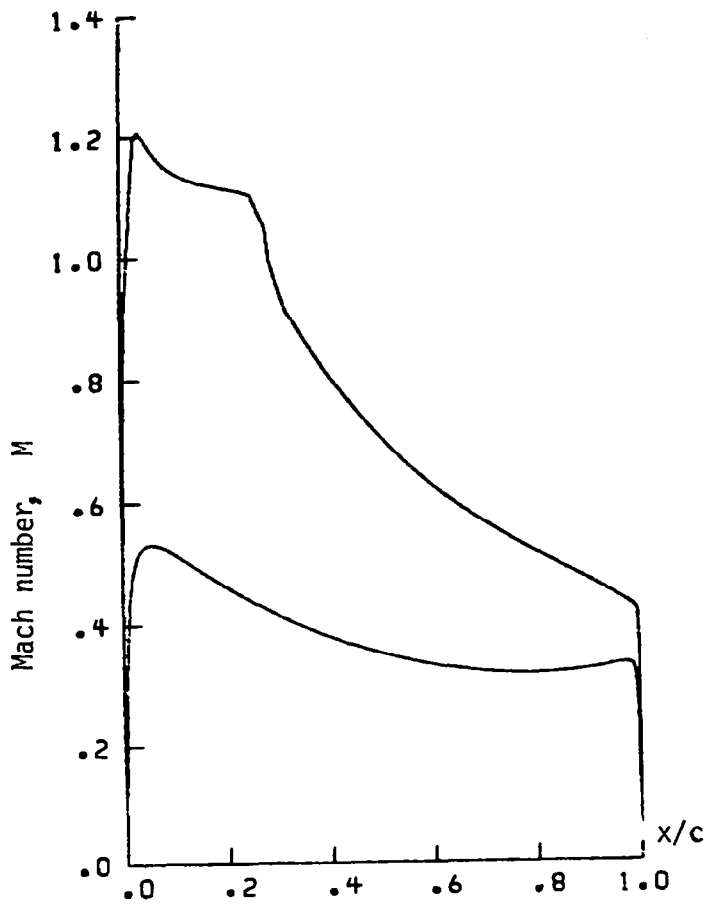


Figure 15. - Test case 1 Mach number distribution for designed shock-free cascade

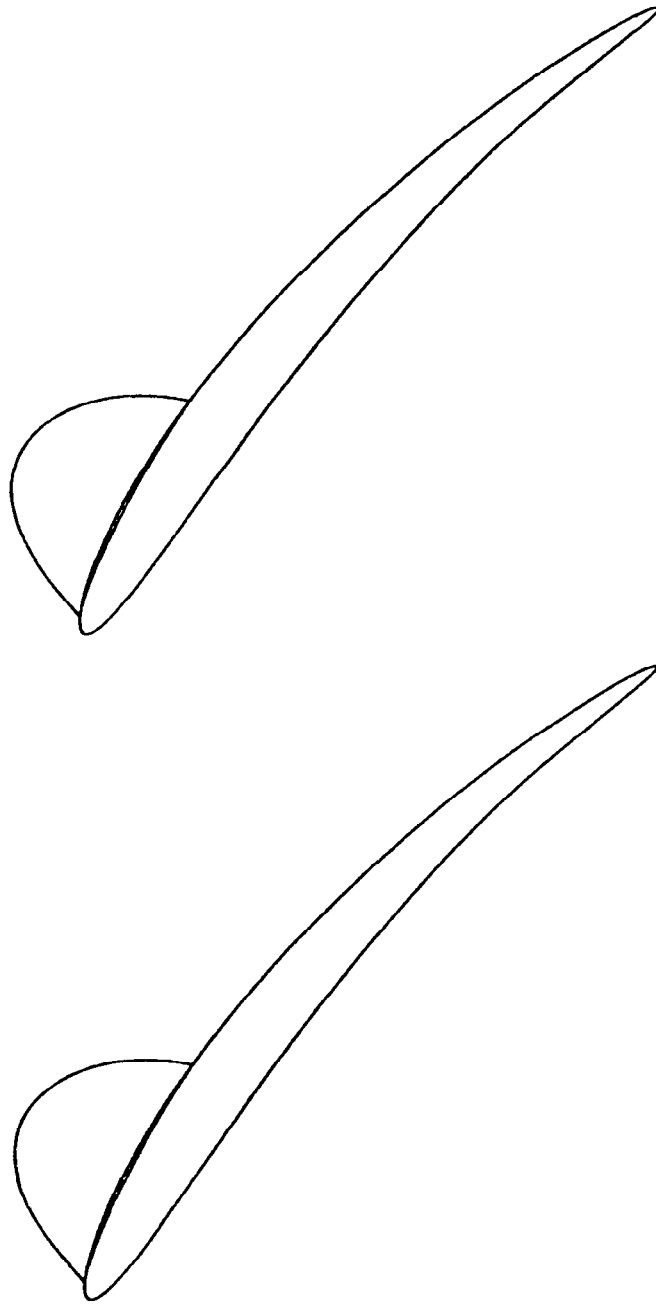


Figure 16. - Test case 1 original and redesigned (shock free) cascade shape with sonic line corresponding to shock-free flow field

```

TEST CASE NO.1 : SHOCKLESS CASCADE
XCELL = 0.24000D+02YCELL = 0.06000D+02PMESH = 4.00000D+00
ALPHA1 = 0.65000D+02TWIST = -0.50000D+02ALPHA2 = 0.42000D+02
PITCH = 0.80000D+00RO1 = 0.00631D+00RO2 = 0.00050D+00
FMACH = 0.80000D+00RLX = 1.75000D+00AR = 1.00000D+00
TITR1 = 2.00000D+02TITR2 = 2.00000D+02TITR3 = 1.00000D+02
TITR4 = 1.00000D+02SUPCEL = 0.98000D+02FACTGAS = 0.00000D+03
POINTS = 1.93000D+02GAMMA = 1.40000D+00CONVER = 1.00000D-09
0.007256 0.000415
0.004287 -0.000482
0.001495 -0.000499
-0.001116 0.000729
-0.003220 0.003425
-0.004654 0.007552
-0.005353 0.013146
-0.005297 0.020307
-0.002388 0.036689
-0.000104 0.044690
0.003308 0.055369
0.008030 0.068782
0.013456 0.083048
0.018302 0.095113
0.026578 0.114652
0.036013 0.114652
0.047030 0.135725
0.059744 0.159113
0.075852 0.182517
0.094740 0.206131
0.083344 0.229191
0.095258 0.249958
0.110253 0.274150
0.113504 0.278982
0.120170 0.288715
0.132350 0.305863
0.144423 0.322303
0.156336 0.338033
0.168051 0.353066
0.179540 0.367424
0.190783 0.381136
0.201771 0.394232
0.212499 0.406749
0.222967 0.418720
0.233176 0.430181
0.243134 0.441163
0.252848 0.451698
0.262327 0.461817
0.271578 0.471547
0.280612 0.480915
0.289439 0.489944
0.298068 0.498657
0.306508 0.507074
0.314770 0.515215
0.322861 0.523097
0.330791 0.530737
0.338568 0.538150
0.346200 0.545349
0.353694 0.552348
0.361059 0.559159
0.368300 0.565792
0.375425 0.572258
0.382440 0.578566
0.389352 0.584726
0.396166 0.590746
0.402887 0.596633
0.409522 0.602396
0.416076 0.608040
0.422553 0.613573
0.428959 0.619000
0.435299 0.624326
0.441576 0.629558
0.447795 0.634700
0.453961 0.639757
0.460077 0.644733
0.466147 0.649633
0.472175 0.654459
0.478165 0.659215
0.484119 0.663904
0.490042 0.668530
0.495935 0.673094
0.501802 0.677599
0.507644 0.682047
0.513465 0.686439
0.519265 0.690776
0.525046 0.695060
0.530810 0.699290
0.536556 0.703467
0.542285 0.707588
0.547996 0.711653
0.553687 0.715660
0.559355 0.719606
0.564999 0.723486
0.570612 0.727297
0.576189 0.731032
0.581722 0.734683
0.587200 0.738242
0.592612 0.741697
0.597942 0.745037
0.603171 0.748244
0.608278 0.751301
0.613235 0.754187
0.618009 0.756875
0.622560 0.759337
0.626844 0.761535
0.630803 0.763430
0.634375 0.764973
0.637485 0.766098
0.640047 0.766747
0.641910 0.766657
0.642787 0.766044

```

Figure 17. - Test case 1 input data set (analysis mode) for shock-free airfoil cascade

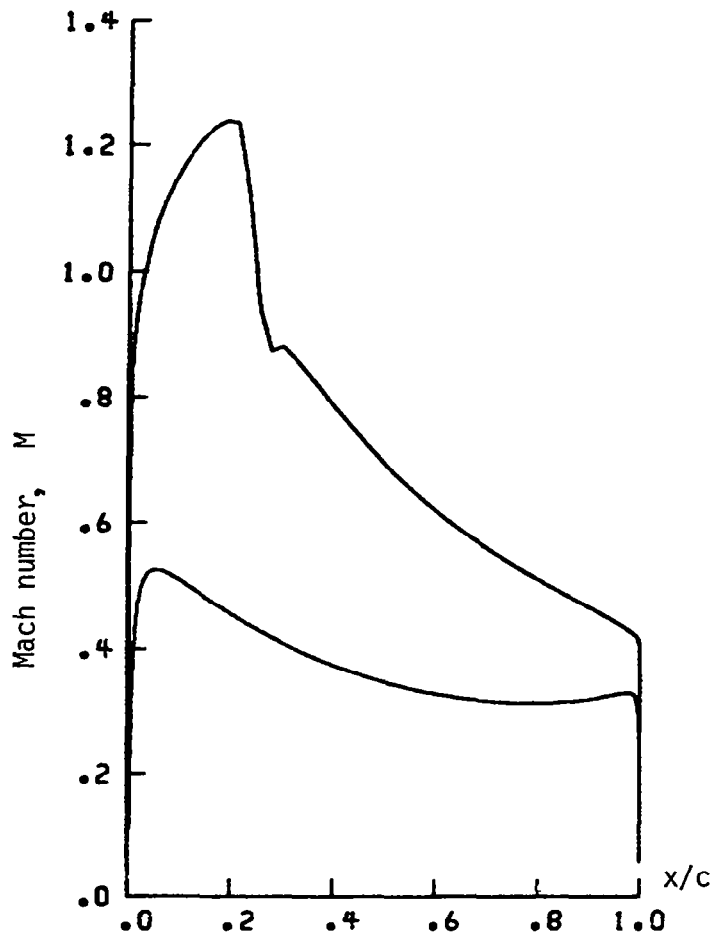


Figure 18. - Test case 1 Mach numbers distribution on original cascade at off-design conditions

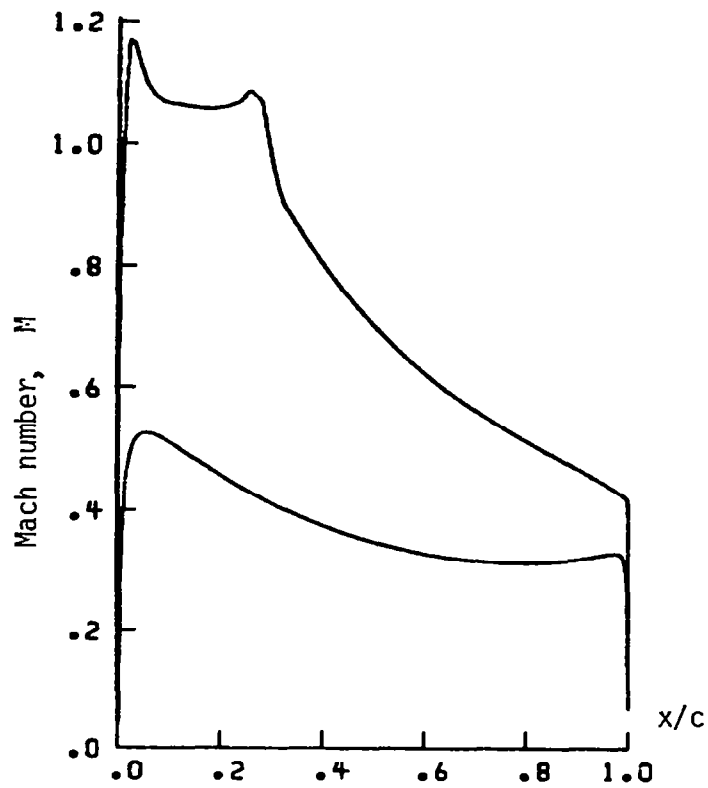


Figure 19. - Test case 1 Mach number distribution on shockless cascade at off-design conditions

```

TEST CASE NO.2 : ORIGINAL CASCADE
XCELL = 0.24000D+02YCELL = 0.06000D+02PMESH = 4.00000D+00
ALPHA1= 0.37000D+02TWIST =-0.27000D+02ALPHA2= 0.16000D+02
PITCH = 1.00000D+00RO1  = 0.00631D+00RO2  = 0.00050D+00
FMACH = 0.72000D+00RLX  = 1.75000D+00AR   = 1.00000D+00
TITR1 = 2.00000D+02TITR2 = 2.00000D+02TITR3 = 1.00000D+02
TITR4 = 1.00000D+02SUPCEL= 0.98000D+02FCTGAS= 0.03000D+03
POINTS= 1.25000D+02GAMMA = 1.40000D+00CONVER= 1.00000D-08
1.000000  0.500000
0.997529  0.496025
0.994917  0.493987
0.992027  0.492139
0.988722  0.490277
0.984871  0.488301
0.980347  0.486147
0.975032  0.483766
0.968815  0.481116
0.961593  0.478160
0.953277  0.474862
0.943784  0.471187
0.933048  0.467099
0.921013  0.462559
0.907637  0.457528
0.892891  0.451963
0.876762  0.445822
0.859250  0.439061
0.840368  0.431636
0.820145  0.423504
0.798623  0.414625
0.775857  0.404961
0.751916  0.394485
0.726879  0.383172
0.700839  0.371010
0.673895  0.357997
0.646161  0.344145
0.617754  0.329479
0.588801  0.314042
0.559433  0.297889
0.529787  0.281096
0.500000  0.263750
0.470213  0.245957
0.440567  0.227834
0.411199  0.209510
0.382246  0.191125
0.353839  0.172824
0.326105  0.154754
0.299161  0.137065
0.273121  0.119900
0.248084  0.103400
0.224143  0.087691
0.201377  0.072889
0.179855  0.059095
0.159632  0.046389
0.140750  0.034835
0.123238  0.024476
0.107109  0.015331
0.092363  0.007401
0.078987  0.000666
0.066952  -0.004914
0.056216  -0.009396
0.046723  -0.012853
0.038407  -0.015368
0.031185  -0.017035
0.024968  -0.017949
0.019653  -0.018202
0.015129  -0.017877
0.011278  -0.017024
0.007973  -0.015641
0.005083  -0.013601
0.002471  -0.010397
0.000000  0.000000
0.002471  0.014347
0.005083  0.021717
0.007973  0.028360
0.011278  0.034993
0.015129  0.041946
0.019653  0.049416
0.024968  0.057523
0.031185  0.066347
0.038407  0.075933
0.046723  0.086300
0.056216  0.097445
0.066952  0.109347
0.078987  0.121970
0.092363  0.135261
0.107109  0.149160
0.123238  0.163592
0.140750  0.178479
0.159632  0.193733
0.179855  0.209265
0.201377  0.224982
0.224143  0.240793
0.248084  0.256607
0.273121  0.272336
0.299161  0.287895
0.326105  0.303207
0.353839  0.318197
0.382246  0.332801
0.411199  0.346957
0.440567  0.360613
0.470213  0.373724
0.500000  0.386250
0.529787  0.398159
0.559433  0.409425
0.588801  0.420028
0.617754  0.429955
0.646161  0.439198
0.673895  0.447755
0.700839  0.455627
0.726879  0.462823
0.751916  0.469354
0.775857  0.475237
0.798623  0.480493
0.820145  0.485145
0.840368  0.489221
0.859250  0.492752
0.876762  0.495770
0.892891  0.498310
0.907637  0.500408
0.921013  0.502103
0.933048  0.503431
0.943784  0.504430
0.953277  0.505139
0.961593  0.505592
0.968815  0.505826
0.975032  0.505873
0.980347  0.505760
0.984871  0.505510
0.988722  0.505136
0.992027  0.504634
0.994917  0.503965
0.997529  0.502983
1.000000  0.500000

```

Figure 20. - Test case 2 input data set (design mode) for original airfoil cascade

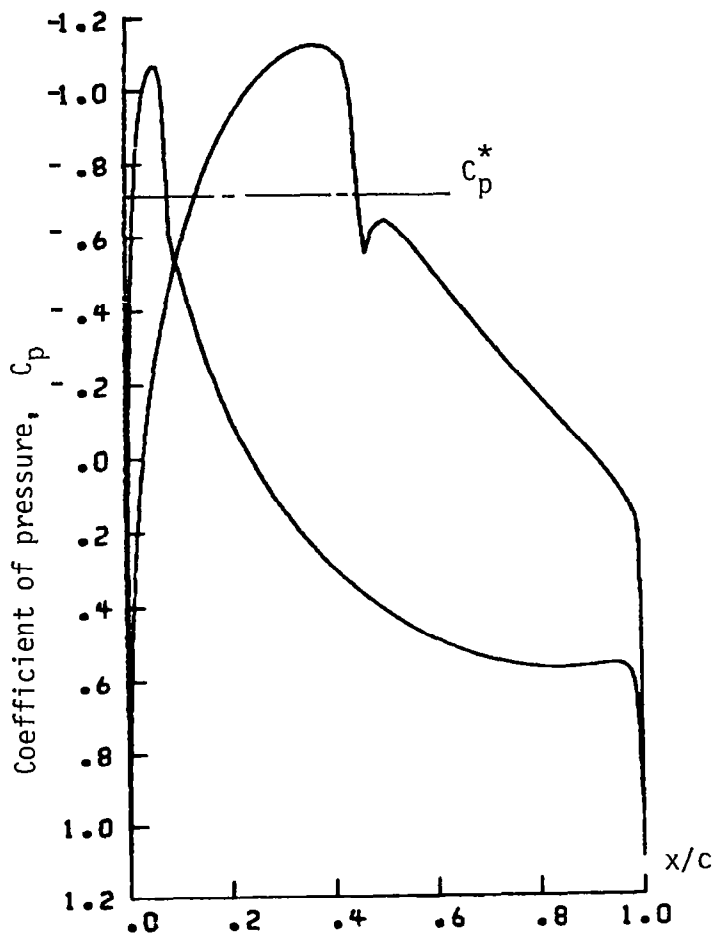


Figure 21. - Test case 2 coefficient-of-pressure distribution on original cascade surface

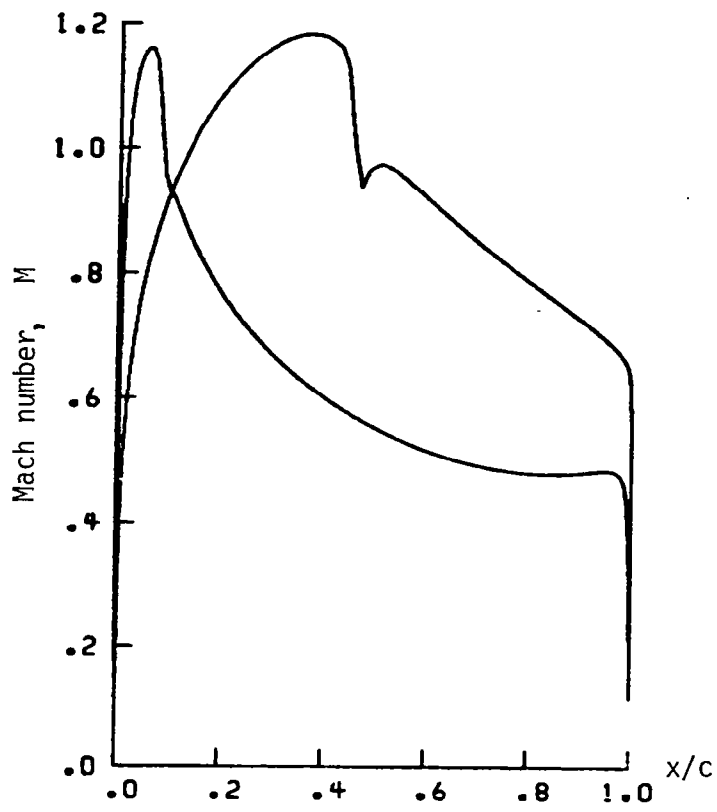


Figure 22. - Test case 2 Mach number distribution on original cascade surface



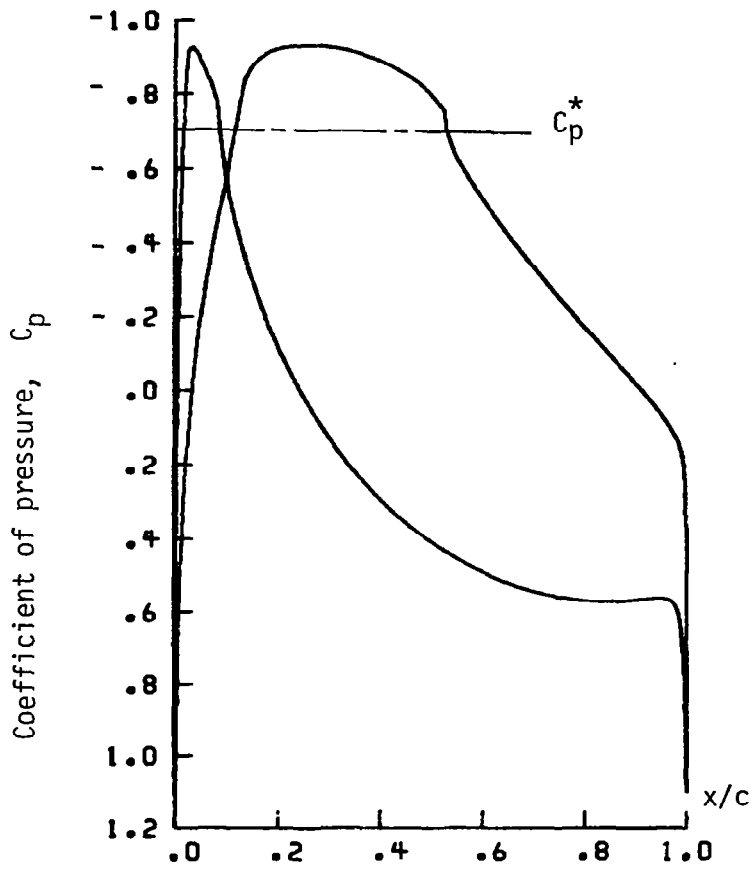


Figure 23. - Test case 2 coefficient-of-pressure distribution on shock-free cascade surface

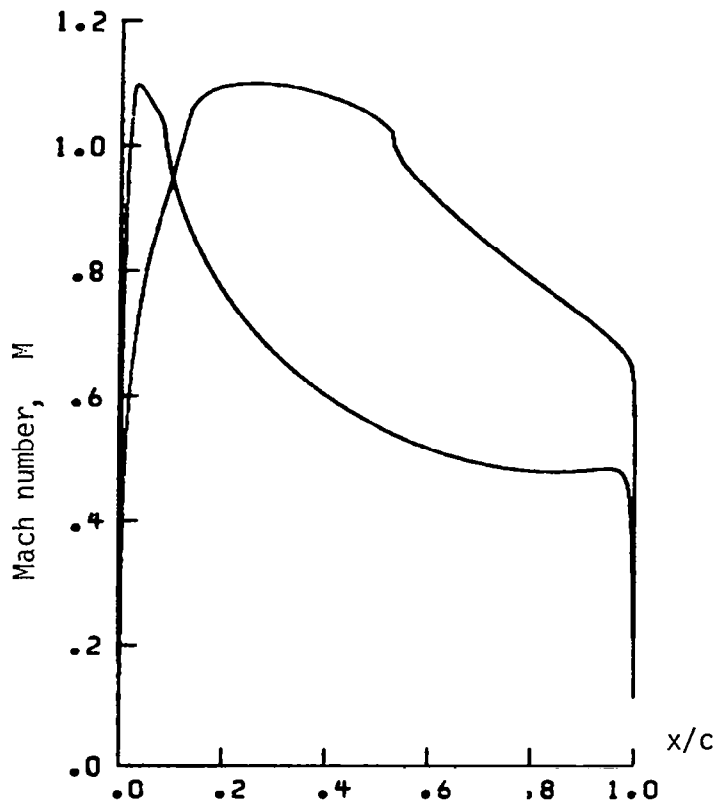


Figure 24. - Test case 2 Mach number distribution on shock-free cascade surface

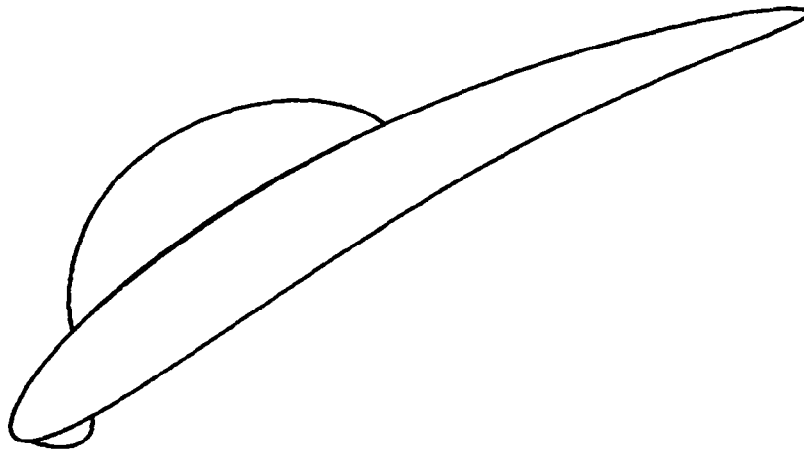
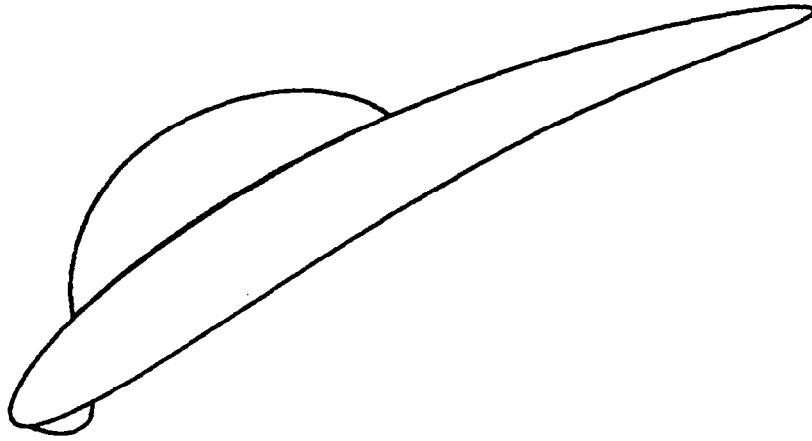


Figure 25. - Test case 2 sonic-line shapes corresponding to shock-free flow field

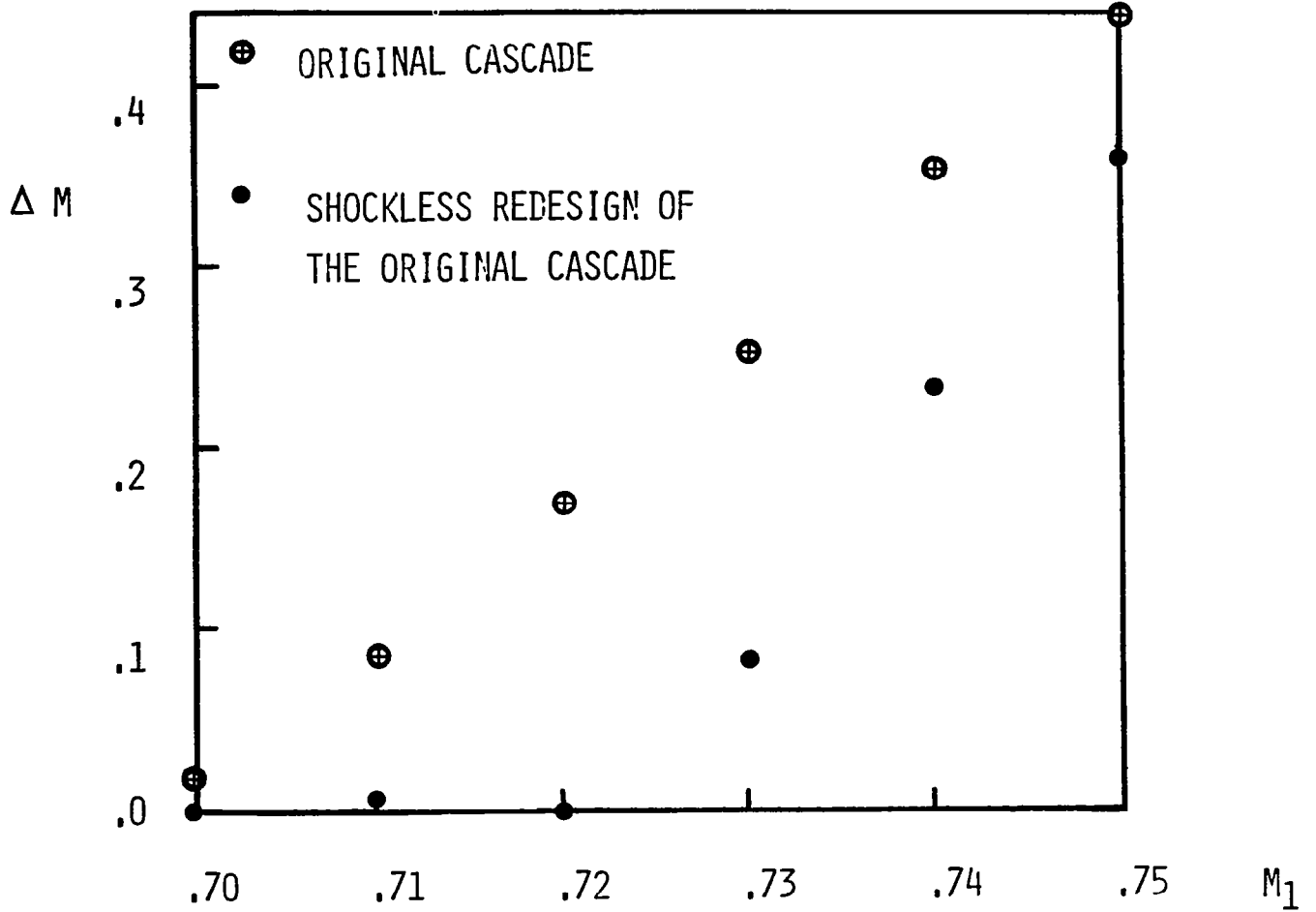


Figure 26. - Test case 2 shock wave losses for original and shock-free cascade over range of free-stream inlet Mach numbers

TEST CASE NO.2 : SHOCKLESS CASCADE		0.005920	-0.005195	
XCELL = 0.24000D+02	YCELL = 0.06000D+02	PMESH = 4.00000D+00	0.003123	-0.003528
ALPHA1 = 0.37000D+02	TWIST = -0.27000D+02	ALPHA2 = 0.16000D+02	0.001138	-0.001629
PITCH = 1.00000D+00	R01 = 0.00631D+00	R02 = 0.00050D+00	-0.000249	0.000444
FMACH = 0.72000D+00	RXL = 1.75000D+00	RAR = 1.00000D+00	-0.001302	0.003028
TITR1 = 2.00000D+02	TITR2 = 2.00000D+02	TITR3 = 1.00000D+02	-0.002013	0.006526
TITR4 = 1.00000D+02	SUPCEL = 0.98000D+02	FCTGAS = 0.00000D+03	-0.002147	0.011032
POINTS = 1.93000D+02	GAMMA = 1.40000D+00	CONVER = 1.00000D-09	-0.001425	0.016424
0.891006	0.453991	0.000201	0.022607	
0.890951	0.453062	0.002730	0.029518	
0.889938	0.451579	0.006179	0.037083	
0.887868	0.449670	0.010537	0.045239	
0.884660	0.447459	0.015785	0.053922	
0.880287	0.444992	0.021894	0.063064	
0.874752	0.442262	0.028829	0.072598	
0.868063	0.439265	0.036545	0.082455	
0.860242	0.435989	0.044995	0.092563	
0.851326	0.432430	0.054124	0.102856	
0.841369	0.428581	0.063876	0.113270	
0.830439	0.424440	0.084053	0.132907	
0.818418	0.420007	0.095096	0.142801	
0.806001	0.415285	0.106861	0.152884	
0.792589	0.410280	0.118669	0.162620	
0.778791	0.405006	0.129606	0.171345	
0.764417	0.399475	0.141927	0.180882	
0.749673	0.393708	0.155557	0.191105	
0.734666	0.387724	0.166493	0.199083	
0.719490	0.381549	0.178186	0.207406	
0.704237	0.375205	0.190525	0.215972	
0.688986	0.368721	0.203417	0.224699	
0.673803	0.362121	0.216941	0.233616	
0.658750	0.355429	0.231001	0.242641	
0.643874	0.348669	0.240727	0.248743	
0.629214	0.341863	0.255748	0.257949	
0.614799	0.335030	0.271327	0.267227	
0.600653	0.328188	0.282057	0.273459	
0.586789	0.321353	0.298383	0.282705	
0.573219	0.314537	0.309671	0.288933	
0.559945	0.307750	0.321167	0.295141	
0.546968	0.301002	0.332634	0.301200	
0.534285	0.294300	0.344182	0.307166	
0.521891	0.287649	0.361552	0.315891	
0.509777	0.281053	0.373012	0.321480	
0.497935	0.274514	0.384370	0.326887	
0.486353	0.268035	0.400703	0.334425	
0.475020	0.261615	0.414626	0.340614	
0.463925	0.255256	0.418407	0.342253	
0.453055	0.248955	0.424014	0.344659	
0.442397	0.242712	0.435888	0.349641	
0.431941	0.236524	0.447671	0.354475	
0.421672	0.230389	0.459364	0.359166	
0.411580	0.224305	0.470969	0.363719	
0.401652	0.218269	0.482488	0.368139	
0.391878	0.212278	0.493923	0.372431	
0.382246	0.206330	0.505275	0.376598	
0.372745	0.200421	0.516548	0.380645	
0.363364	0.194547	0.527743	0.384576	
0.354095	0.188707	0.538862	0.388394	
0.344927	0.182897	0.549907	0.392103	
0.335851	0.177115	0.560880	0.395705	
0.326858	0.171357	0.571783	0.399204	
0.317941	0.165621	0.582617	0.402602	
0.309090	0.159904	0.593385	0.405900	
0.300300	0.154204	0.604086	0.409102	
0.291561	0.148519	0.614723	0.412208	
0.282869	0.142848	0.625296	0.415220	
0.274215	0.137190	0.635805	0.418141	
0.265594	0.131542	0.646250	0.420970	
0.257003	0.125903	0.656631	0.423708	
0.248434	0.120274	0.666947	0.426357	
0.239884	0.114656	0.677196	0.428915	
0.231349	0.109048	0.687376	0.431384	
0.222825	0.103453	0.697485	0.433763	
0.214310	0.097872	0.707518	0.436052	
0.205803	0.092307	0.717472	0.438249	
0.197301	0.086762	0.727341	0.440353	
0.188805	0.081241	0.737118	0.442363	
0.180314	0.075751	0.746795	0.444277	
0.171830	0.070297	0.756364	0.446094	
0.163356	0.064887	0.765814	0.447811	
0.154895	0.059530	0.775132	0.449425	
0.146453	0.054235	0.784304	0.450933	
0.138034	0.049015	0.793315	0.452331	
0.129647	0.043884	0.802144	0.453615	
0.121301	0.038856	0.810773	0.454783	
0.113006	0.033950	0.819175	0.455829	
0.104776	0.029183	0.827326	0.456747	
0.096625	0.024577	0.835194	0.457533	
0.088571	0.020156	0.842747	0.458182	
0.080322	0.019494	0.849947	0.458687	
0.082936	0.017194	0.856755	0.459040	
0.072747	0.012118	0.863125	0.459236	
0.064570	0.008280	0.869009	0.459267	
0.057465	0.005123	0.874354	0.459123	
0.050269	0.002119	0.879106	0.458793	
0.043462	-0.000506	0.883201	0.458264	
0.036620	-0.002881	0.886570	0.457510	
0.030488	-0.004709	0.889112	0.456482	
0.018957	-0.006869	0.890614	0.455130	
0.013948	-0.006949	0.891006	0.453991	
0.009562	-0.006382			

Figure 27. - Test case 2 input data set (analysis mode) for shock-free airfoil cascade

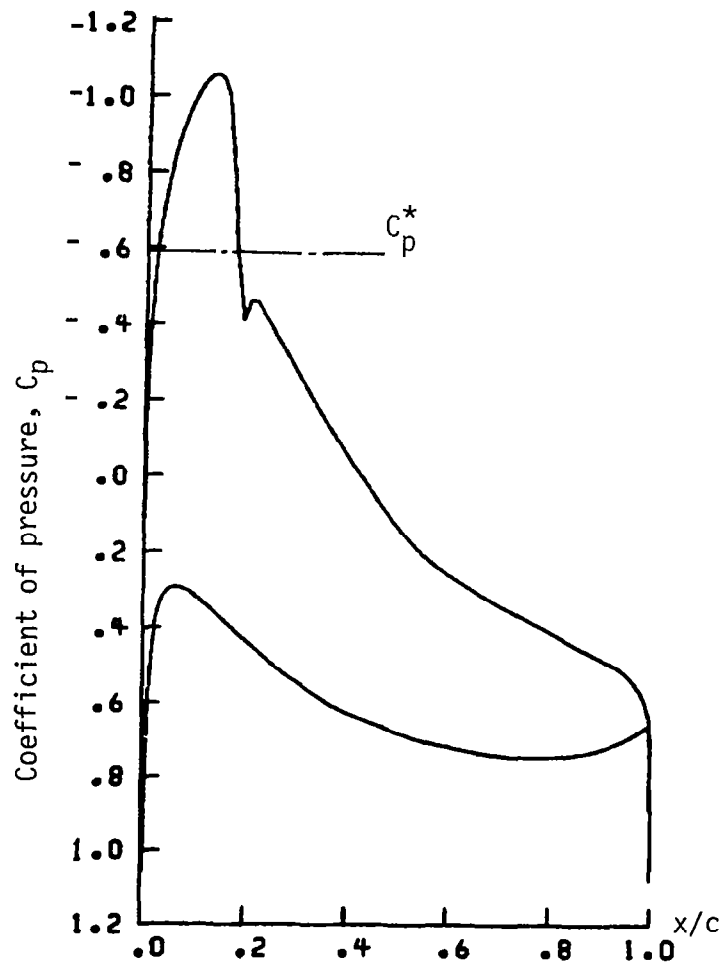


Figure 28. - Test case 3 coefficient of pressure distribution on original cascade surface

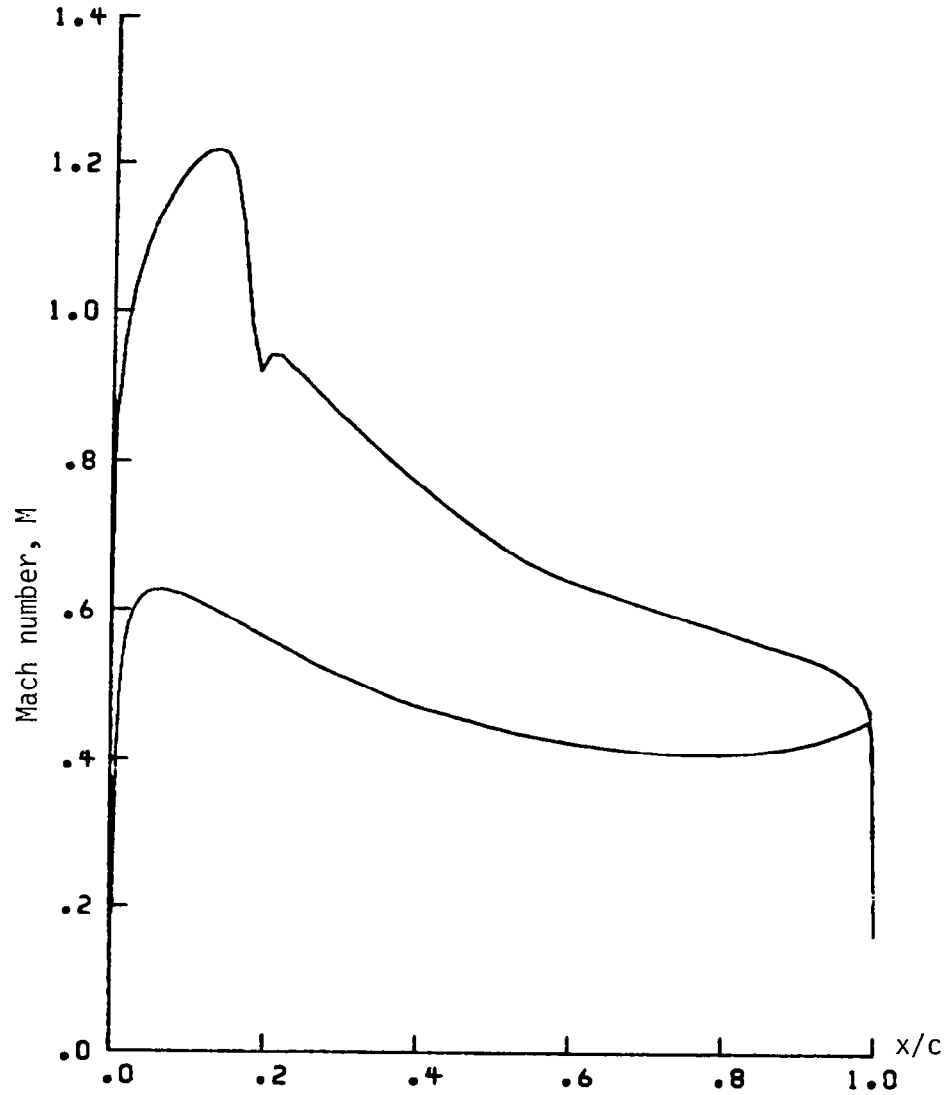


Figure 29. - Test case 3 Mach number distribution on original cascade surface

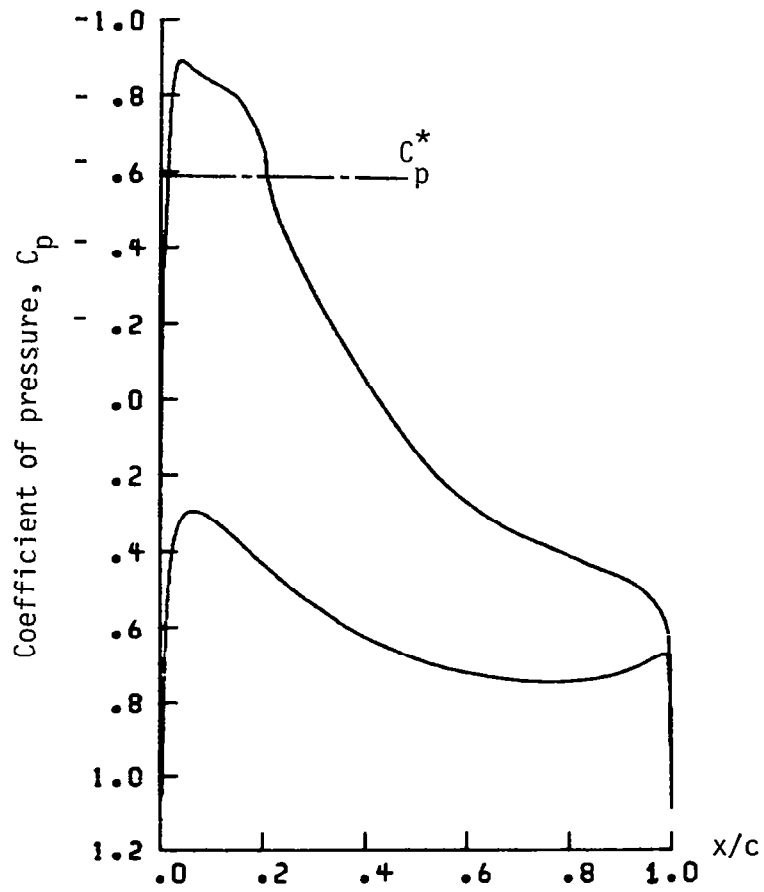


Figure 30. - Test case 3 coefficient-of-pressure distribution on shock-free cascade surface



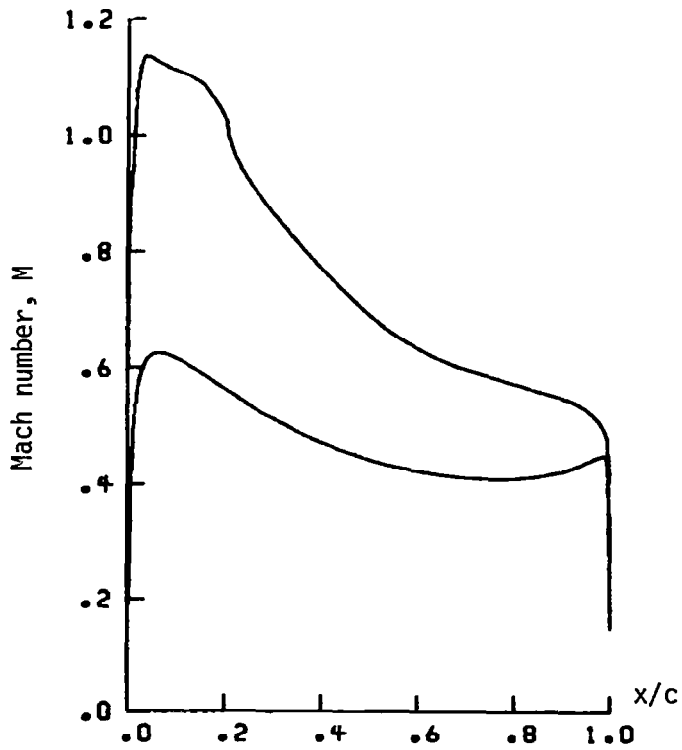
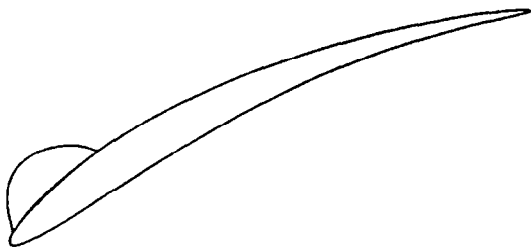
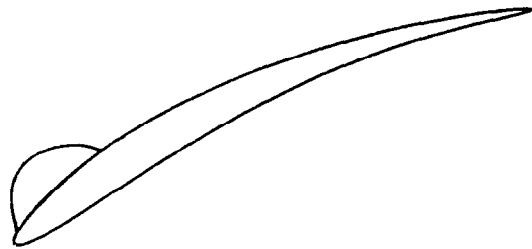


Figure 31. - Test case 3 Mach number distribution on shock-free cascade surface

```

TEST CASE NO.3 : ORIGINAL CASCADE
XCELL = 0.24000D+02YCELL = 0.05000D+02PMESH = 4.00000D+00
ALPHA1= 0.45500D+02TWIST =-0.25000D+02ALPHA2= 0.13500D+02
FITCH = 0.66566D+00RO1 = 0.00631D+00RO2 = 0.00100D+00
FMACH = 0.75000D+00RLX = 1.72000D+00AR = 1.00000D+00
TITR1 = 2.00000D+02TITR2 = 2.00000D+02TITR3 = 1.00000D+02
TITP4 = 1.00000D+02SUPCEL= 0.98000D+02FCTGAS= 0.02000D+03
FOIKTS= 1.25000D+02GAMMA = 1.40000D+00CONVER= 1.00000D-09
1.000000 0.516100
0.997529 0.514072
0.994917 0.512904
0.992027 0.511795
0.988722 0.510639
0.984871 0.509376
0.980347 0.507964
0.975032 0.506365
0.968315 0.504546
0.961593 0.502476
0.953277 0.500119
0.943284 0.497444
0.933048 0.494414
0.921013 0.490990
0.907637 0.487132
0.892891 0.482796
0.876762 0.477935
0.859250 0.472502
0.840368 0.466448
0.819014 0.459722
0.792623 0.452275
0.775957 0.444062
0.751916 0.435040
0.726979 0.425173
0.700839 0.414432
0.673395 0.402799
0.646161 0.390266
0.617754 0.376840
0.588901 0.362541
0.559433 0.347405
0.529787 0.331485
0.500000 0.314849
0.470213 0.297582
0.440567 0.279785
0.411199 0.261570
0.382246 0.243063
0.353839 0.224401
0.326105 0.205725
0.299161 0.187182
0.273121 0.168920
0.248084 0.151084
0.224143 0.133814
0.201377 0.117240
0.179855 0.101485
0.159632 0.086652
0.140750 0.072832
0.123238 0.060097
0.107109 0.048500
0.092363 0.038072
0.078957 0.028825
0.064952 0.020752
0.056216 0.013823
0.046723 0.007994
0.038407 0.003202
0.031185 -0.000630
0.024968 -0.003586
0.019453 -0.005757
0.015129 -0.007231
0.011278 -0.008083
0.007973 -0.008350
0.005083 -0.007985
0.002471 -0.006666
0.000000 0.000000
0.002471 0.011569
0.005083 0.018018
0.007973 0.024013
0.011278 0.030130
0.015129 0.036655
0.019653 0.043766
0.024968 0.051582
0.031185 0.060179
0.038407 0.069606
0.046723 0.079881
0.056216 0.091002
0.066952 0.102944
0.078987 0.115665
0.092363 0.129108
0.107109 0.143201
0.123238 0.157865
0.140750 0.173007
0.159632 0.188533
0.179855 0.204343
0.201377 0.220338
0.224143 0.236418
0.248084 0.252488
0.273121 0.268456
0.299161 0.284237
0.326105 0.299753
0.353839 0.314932
0.382246 0.329712
0.411199 0.344036
0.440567 0.357860
0.470213 0.371141
0.500000 0.383849
0.529787 0.395957
0.559433 0.407446
0.588801 0.418301
0.617754 0.428515
0.646161 0.438081
0.673895 0.447002
0.700839 0.455280
0.726879 0.462923
0.751916 0.469944
0.775857 0.476356
0.798623 0.482177
0.820145 0.487429
0.840368 0.492134
0.859250 0.496317
0.876762 0.500008
0.892891 0.503235
0.907637 0.506030
0.921013 0.508425
0.933048 0.510453
0.943784 0.512146
0.953277 0.513538
0.961593 0.514662
0.968815 0.515550
0.975032 0.516231
0.980347 0.516735
0.984871 0.517088
0.988722 0.517309
0.992027 0.517413
0.994917 0.517397
0.997529 0.517209
1.000000 0.516100

```

Figure 32. - Test case 3 input data set (design mode) for original airfoil cascade

```

TEST CASE NO. 3 : SHOCKLESS CASCADE
XCELL = 0.24000D+02YCELL = 0.05000D+02PMESH = 4.00000D+00
ALPHA1 = 0.45500D+02TWIST = -0.25000D+02ALPHA2 = 0.13500D+02
PITCH = 0.66666D+00R01 = 0.00631D+00R02 = 0.00100D+00
FMACH = 0.75000D+00RLX = 1.72000D+00AK = 1.00000D+00
TITR1 = 2.00000D+02TITR2 = 2.00000D+02TITR3 = 1.00000D+02
TITR4 = 1.00000D+02SUPCEL = 0.98000D+02FCTGAS = 0.00000D+03
POINTS = 1.93000D+02GAMMA = 1.40000D+00CONVER = 1.00000D-09
0.906307 0.422019
0.903057 0.420487
0.899322 0.419212
0.895492 0.418072
0.891556 0.416935
0.887497 0.415945
0.883294 0.414897
0.878924 0.413835
0.874363 0.412749
0.869590 0.411625
0.864580 0.410455
0.859313 0.409230
0.853767 0.407963
0.847925 0.406583
0.841768 0.405144
0.835279 0.403615
0.828445 0.401990
0.821250 0.400260
0.813684 0.398415
0.805737 0.396447
0.797402 0.394366
0.788671 0.392104
0.779542 0.389711
0.770012 0.387158
0.760081 0.384436
0.749752 0.381534
0.739027 0.378444
0.727913 0.375157
0.716419 0.371665
0.704553 0.367960
0.692329 0.364033
0.679758 0.359878
0.666857 0.355490
0.653642 0.350863
0.640133 0.345993
0.626347 0.340878
0.612308 0.335517
0.598036 0.329908
0.583556 0.324054
0.568890 0.317958
0.554064 0.311625
0.539103 0.305059
0.524033 0.298269
0.508879 0.291263
0.493667 0.284054
0.478424 0.276651
0.463175 0.269071
0.447944 0.261325
0.432759 0.253432
0.417642 0.245408
0.402618 0.237271
0.387710 0.229040
0.372939 0.220734
0.358329 0.212373
0.343899 0.203977
0.329668 0.195569
0.315656 0.187167
0.301879 0.178793
0.288355 0.170467
0.275098 0.162209
0.262122 0.154038
0.249441 0.145974
0.237066 0.138034
0.225007 0.130237
0.213274 0.122597
0.201875 0.115130
0.190817 0.107850
0.180105 0.100771
0.169743 0.093905
0.159736 0.087260
0.150083 0.080846
0.140787 0.074670
0.131846 0.068739
0.123258 0.063057
0.115021 0.057627
0.107129 0.052452
0.099577 0.047531
0.092358 0.042865
0.085464 0.038449
0.078885 0.034281
0.072611 0.030357
0.066630 0.026672
0.060928 0.023218
0.055491 0.019990
0.050302 0.016979
0.045346 0.014178
0.040602 0.011581
0.036051 0.009180
0.031672 0.006971
0.027439 0.004953
0.023328 0.003128
0.019310 0.001509
0.015352 0.000122
0.011420 -0.000973
0.007480 -0.001648
0.003547 -0.001587
0.000000 -0.000001
-0.001734 0.003597
-0.001802 0.007851
-0.000901 0.011884
0.000590 0.015800
0.002346 0.019747
0.006621 0.027696
0.008981 0.031440
0.011505 0.035156
0.014603 0.039442
0.017761 0.043599
0.021362 0.048154
0.024681 0.052213
0.028456 0.056696
0.031563 0.060296
0.037000 0.066435
0.043151 0.073169
0.047714 0.078041
0.052714 0.083271
0.060644 0.091352
0.066250 0.096924
0.072157 0.102677
0.078283 0.108521
0.087553 0.117143
0.097028 0.125682
0.103559 0.131414
0.113765 0.140120
0.124194 0.148699
0.134189 0.156622
0.147757 0.166883
0.149265 0.167981
0.158616 0.174684
0.170146 0.182694
0.182113 0.190748
0.194506 0.198827
0.207316 0.206914
0.220526 0.214989
0.234121 0.223034
0.240034 0.231031
0.262395 0.238964
0.277032 0.246814
0.291973 0.254567
0.307192 0.262208
0.322663 0.269721
0.338359 0.277096
0.354253 0.284319
0.370314 0.291350
0.386512 0.298270
0.402817 0.304980
0.419199 0.311502
0.435624 0.317830
0.452064 0.323959
0.468485 0.329885
0.484857 0.335604
0.501149 0.341114
0.517333 0.346414
0.533377 0.351501
0.549255 0.356378
0.564938 0.361043
0.580400 0.365498
0.595617 0.369745
0.610562 0.373786
0.625216 0.377625
0.639556 0.381263
0.653563 0.384706
0.667220 0.387957
0.680511 0.391022
0.693421 0.393905
0.705938 0.396610
0.718052 0.399144
0.729756 0.401512
0.741040 0.403721
0.751900 0.405776
0.762337 0.407683
0.772348 0.409449
0.781932 0.411081
0.791097 0.412585
0.799845 0.413967
0.808184 0.415234
0.816123 0.416392
0.823673 0.417449
0.830849 0.418409
0.837662 0.419280
0.844129 0.420066
0.850269 0.420774
0.856100 0.421407
0.861644 0.421971
0.866920 0.422469
0.871955 0.422906
0.876772 0.423282
0.881395 0.423598
0.885852 0.423852
0.890168 0.424039
0.894373 0.424142
0.898493 0.424135
0.902554 0.423936
0.906307 0.422619

```

Figure 33. - Test case 3 input data set for shock-free cascade

```

TEST CASE NO.4 : NACA0018 ORIGINAL CASCADE
XCELL = 0.24000D+02YCELL = 0.05000D+02PMESH = 4.00000D+00
ALPHA1= 0.00000D+02TWIST = 0.00000D+02ALPHA2= 0.00000D+02
PITCH = 1.00000D+00R01 = 0.01580D+00R02 = 0.00050D+00
FMACH = 0.58200D+00RLX = 1.70000D+00AR = 1.00000D+00
TITR1 = 2.00000D+02TITR2 = 2.00000D+02TITR3 = 1.00000D+02
TITR4 = 2.00000D+02SUPCEL = 1.98000D+02FCTGAS= 5.00000D+02
POINTS= 0.64000D+02GAMMA = 1.40000D+00CONVER= 1.00000D-08
1.000000 0.000000
0.991149 -0.001873
0.988699 -0.002388
0.986111 -0.002930
0.983246 -0.003528
0.979970 -0.004210
0.976153 -0.005000
0.971670 -0.005924
0.966402 -0.007002
0.960239 -0.008256
0.953082 -0.009699
0.944839 -0.011347
0.935430 -0.013207
0.924789 -0.015286
0.912861 -0.017586
0.899603 -0.020104
0.884988 -0.022834
0.869002 -0.025768
0.851644 -0.028891
0.832929 -0.032189
0.812285 -0.035641
0.791554 -0.039225
0.768990 -0.042917
0.745260 -0.046688
0.720445 -0.050510
0.694635 -0.054351
0.667930 -0.058176
0.640441 -0.061951
0.612286 -0.065638
0.583589 -0.069197
0.554482 -0.072589
0.525097 -0.075772
0.495574 -0.078707
0.466051 -0.081353
0.436667 -0.083672
0.407559 -0.085626
0.378862 -0.087185
0.350707 -0.088319
0.323218 -0.089005
0.296513 -0.089229
0.270703 -0.088980
0.245228 -0.088256
0.222159 -0.087065
0.199595 -0.085418
0.178263 -0.083339
0.158219 -0.080855
0.139504 -0.077999
0.122147 -0.074813
0.106161 -0.071340
0.091546 -0.067626
0.078288 -0.063720
0.066359 -0.059672
0.055718 -0.055529
0.046310 -0.051337
0.038067 -0.047138
0.030909 -0.042967
0.024747 -0.038851
0.019479 -0.034800
0.014995 -0.030805
0.011178 -0.026819
0.007902 -0.022733
0.005038 -0.018302
0.002449 -0.012886
0.000000 0.000000

```

Figure 34. - Test case 4 input data set  
(design mode) for choked cascade of  
NACA 0018 airfoils

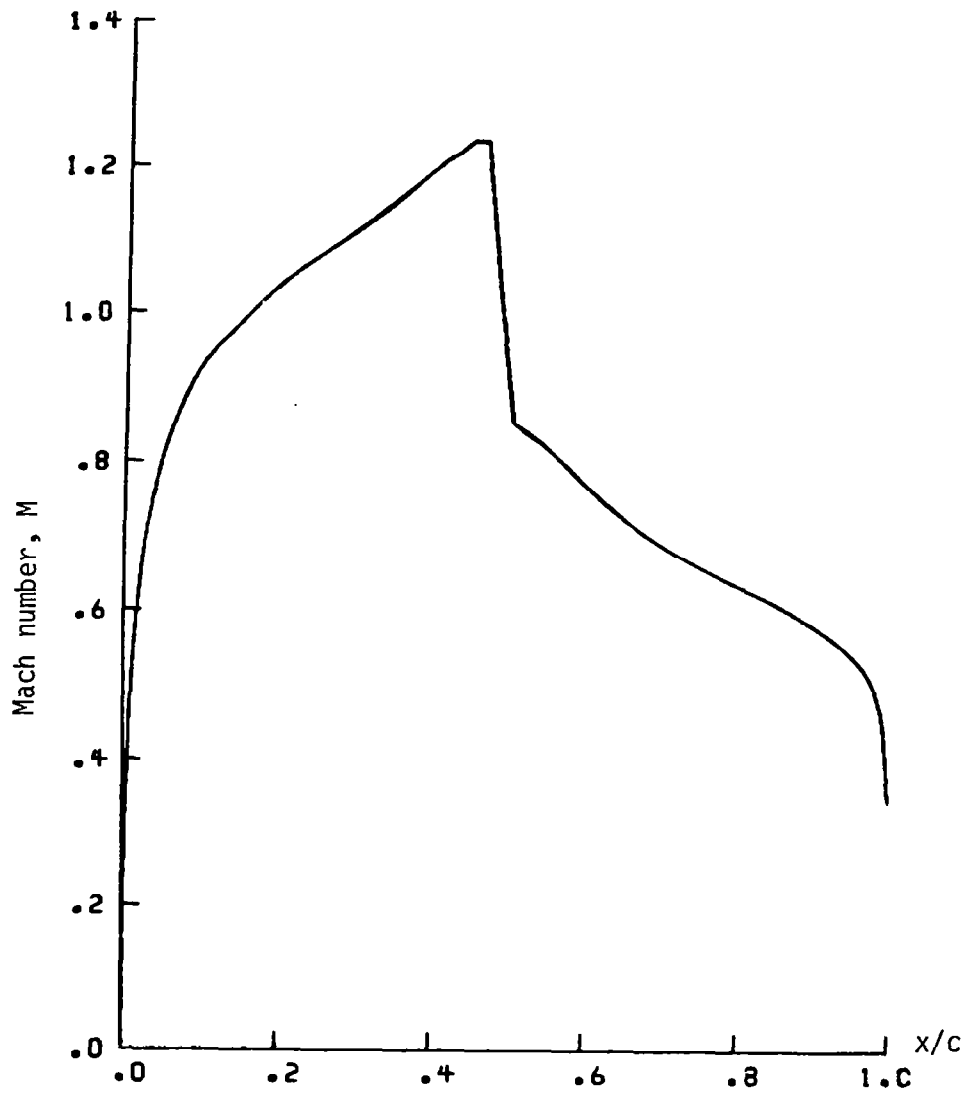


Figure 35. - Test case 4 Mach number distribution on original choked cascade of NACA 0018 airfoils

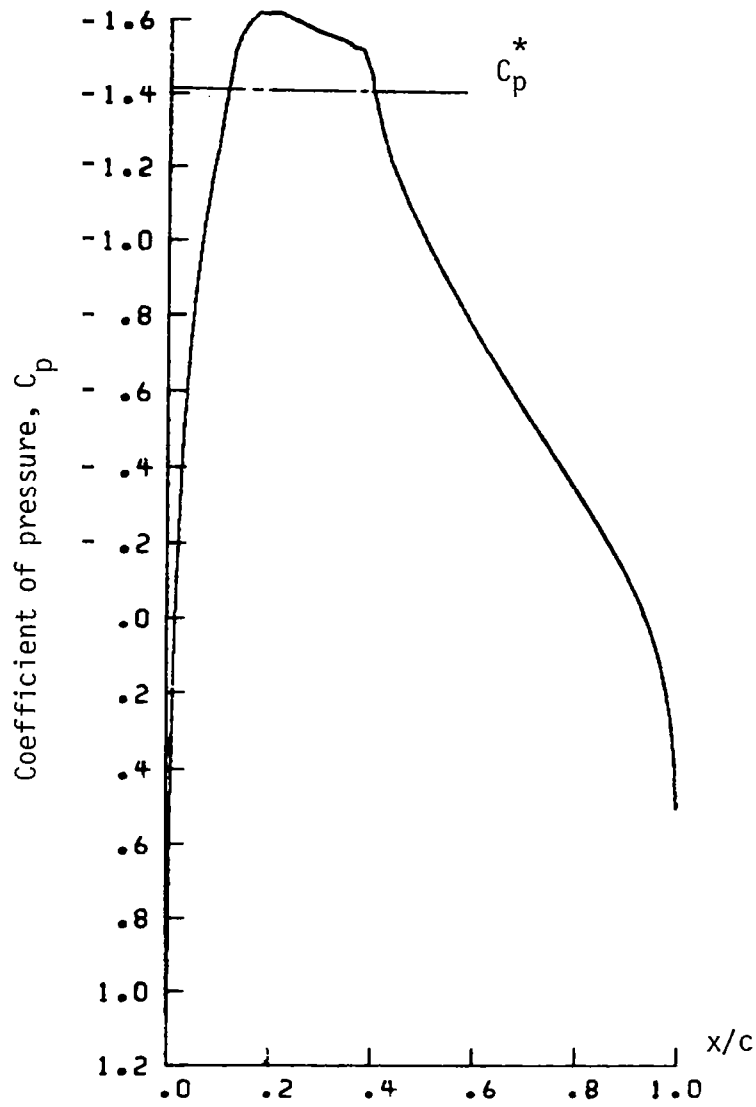


Figure 36. - Test case 4 coefficient-of-pressure distribution on shock-free unchoked cascade of originally NACA 0018 airfoils

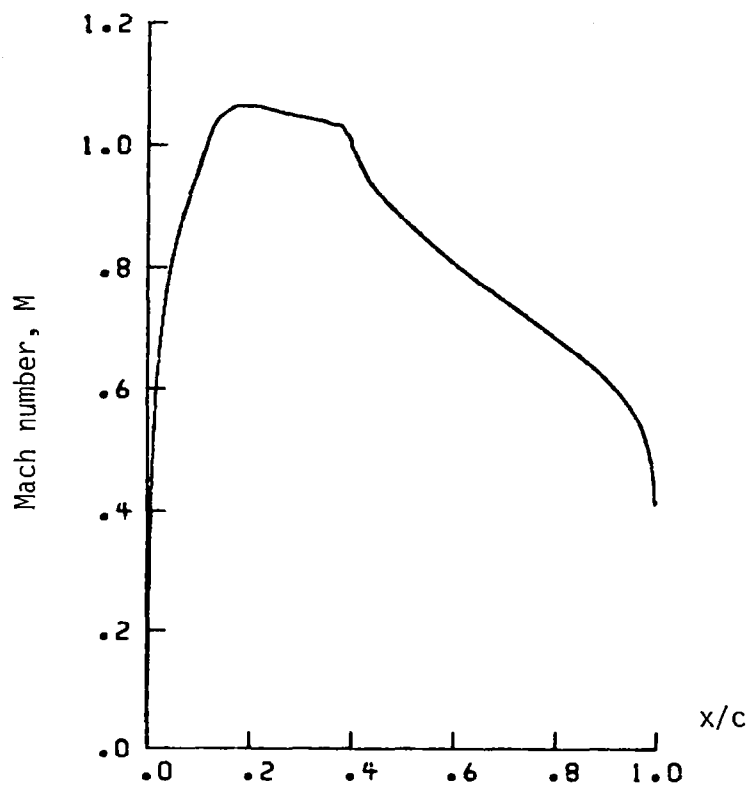


Figure 37. - Test case 4 Mach number distribution on shock-free unchoked cascade surface of modified NACA 0018 airfoils

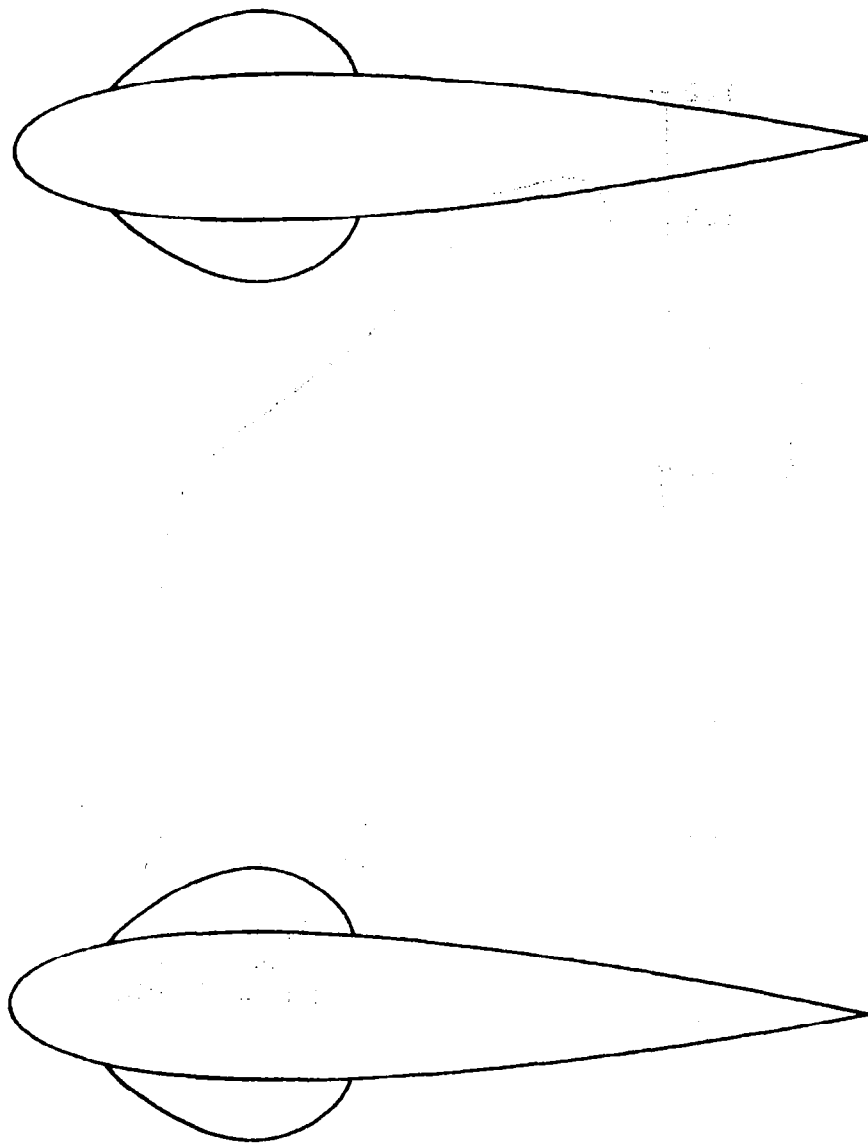


Figure 38. - Test case 4 sonic line shapes for shock-free unchoked cascade of originally NACA 0018 airfoils



```

TEST CASE NO.4 : NACA0018 SHOCKLESS CASCADE
XCELL = 0.240000D+02YCELL = 0.050000D+02PMESH = 4.000000D+00
ALPHA1= 0.000000D+02TWIST =-0.000000D+02ALPHA2= 0.000000D+02
PITCH = 1.000000D+00R01 = 0.015800D+00R02 = 0.000500D+00
FMACH = 0.582000D+00RLX = 1.700000D+00AR = 1.000000D+00
TITR1 = 2.000000D+02TITR2 = 2.000000D+02TITR3 = 1.000000D+02
TITR4 = 2.000000D+02SUPCEL = 1.980000D+02FCTGAS= 0.000000D+02
POINTS= 0.960000D+02GAMMA = 1.400000D+00CONVER= 1.000000D+00
1.000000 -0.000000
0.993426 -0.001393
0.990060 -0.002102
0.986600 -0.002828
0.983016 -0.003576
0.979277 -0.004354
0.975355 -0.005165
0.971219 -0.006017
0.966844 -0.006912
0.962201 -0.007858
0.957266 -0.008857
0.952013 -0.009914
0.946420 -0.011032
0.940466 -0.012215
0.934129 -0.013463
0.927391 -0.014780
0.920236 -0.016168
0.912648 -0.017627
0.904614 -0.019157
0.896122 -0.020759
0.887163 -0.022431
0.877730 -0.024173
0.867816 -0.025934
0.857418 -0.027859
0.846536 -0.029799
0.835168 -0.031799
0.823319 -0.033855
0.810991 -0.035964
0.798194 -0.038120
0.784934 -0.040319
0.771222 -0.042557
0.757072 -0.044826
0.742497 -0.047120
0.727514 -0.049435
0.712140 -0.051761
0.696396 -0.054094
0.680301 -0.056423
0.663880 -0.058743
0.647156 -0.061045
0.630155 -0.063320
0.612902 -0.065560
0.595425 -0.067754
0.577753 -0.069896
0.559916 -0.071974
0.541942 -0.073979
0.523865 -0.075901
0.505713 -0.077731
0.487519 -0.079459
0.469315 -0.081075
0.451132 -0.082572
0.433004 -0.083937
0.414961 -0.085163
0.397601 -0.086208
0.379580 -0.086295
0.377012 -0.087109
0.360634 -0.087620
0.342480 -0.088007
0.324821 -0.088224
0.306722 -0.088284
0.291385 -0.088208
0.274850 -0.087986
0.259361 -0.087640
0.243332 -0.087125
0.229061 -0.086517
0.214633 -0.085738
0.200697 -0.084819
0.187553 -0.083768
0.173663 -0.082438
0.160694 -0.080966
0.148272 -0.079307
0.136655 -0.077501
0.125511 -0.075503
0.104949 -0.071053
0.095174 -0.068602
0.085929 -0.066040
0.077213 -0.063378
0.069021 -0.060625
0.061348 -0.057791
0.054188 -0.054885
0.047532 -0.051914
0.041369 -0.048889
0.035639 -0.045814
0.030478 -0.042697
0.025725 -0.039544
0.021417 -0.036359
0.017539 -0.033145
0.014080 -0.029907
0.011027 -0.026646
0.008358 -0.023366
0.006096 -0.020066
0.004196 -0.016752
0.002663 -0.013425
0.001490 -0.010078
0.000662 -0.006720
0.000167 -0.003360
0.000000 -0.000000

```

Figure 39. - Test case 4 input data set (analysis mode) for a shock-free unchoked cascade of an originally choked cascade

of NACA 0018 airfoils

(85, 55, 100) newton noisupo refuB and aboo SS2A0 to sbom

— Shockless design mode of CAS22 code  
 - - - Analysis mode of CAS22 code  
 - · - Analysis with an Euler solver

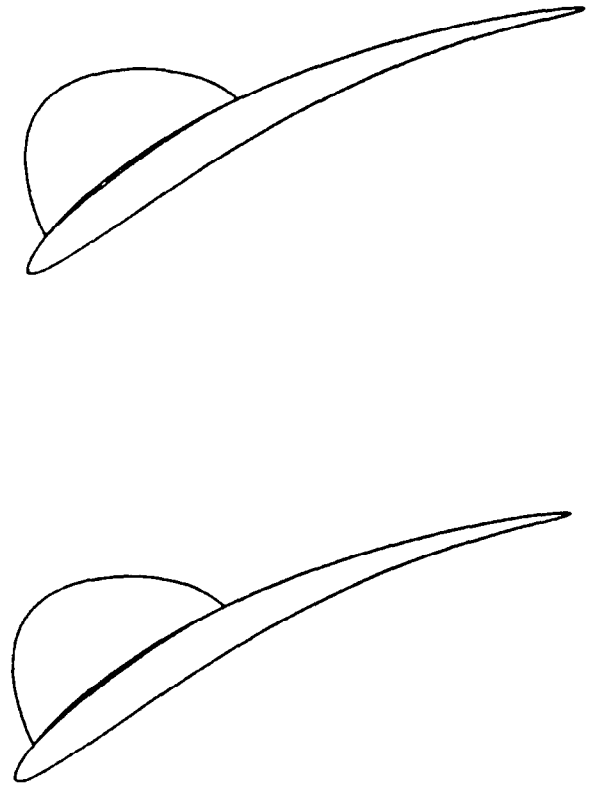
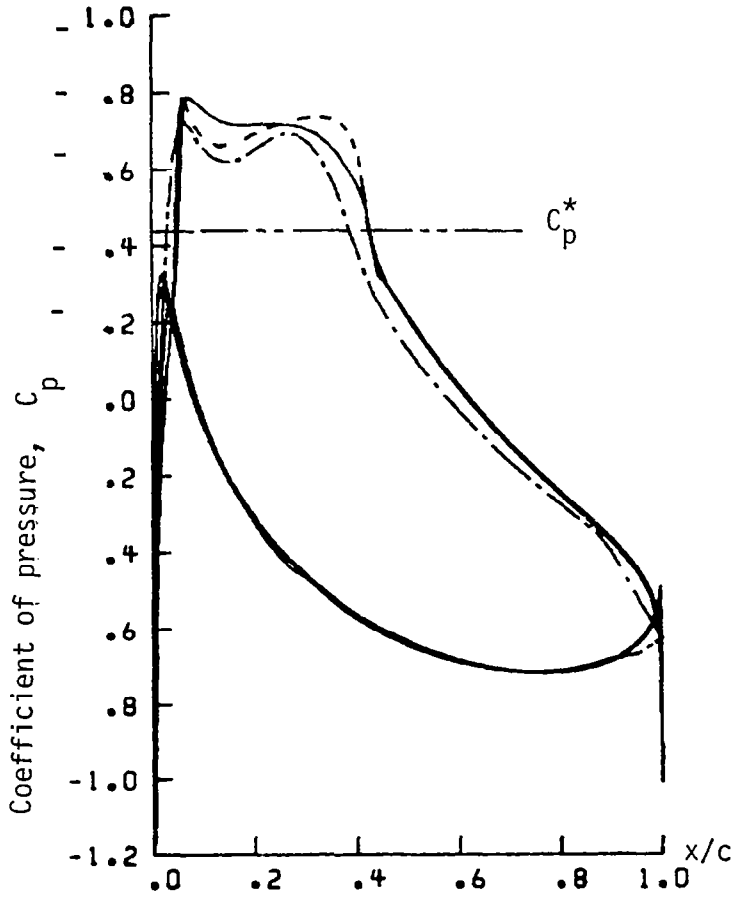


Figure 40.- Comparison of results of exact shock-free design with results of analysis mode of CAS22 code and Euler equation solver (ref. 27,28)

1. Report No. NASA CR-3507	2. Government Accession No.	3. Recipient's Catalog No.	
4. Title and Subtitle <b>CAS22 - FORTRAN PROGRAM FOR FAST DESIGN AND ANALYSIS OF SHOCK-FREE AIRFOIL CASCADES USING FICTITIOUS-GAS CONCEPT</b>		5. Report Date January 1982	6. Performing Organization Code
		8. Performing Organization Report No. <b>None</b>	
7. Author(s) <b>Djordje S. Dulikravich and Helmut Sobieczky</b>		10. Work Unit No.	
9. Performing Organization Name and Address <b>Universities Space Research Association American City Bldg., Suite 311 Columbia, Maryland 21044</b>		11. Contract or Grant No. <b>NAS3-22532</b>	
		13. Type of Report and Period Covered <b>Contractor Report</b>	
12. Sponsoring Agency Name and Address <b>National Aeronautics and Space Administration Washington, D.C. 20546</b>		14. Sponsoring Agency Code <b>505-32-52</b>	
		15. Supplementary Notes <b>Final report. Project Manager, W. D. McNally, Fluid Mechanics and Acoustics Division, NASA Lewis Research Center, Cleveland, Ohio 44135.</b>	
16. Abstract A user-oriented computer program, CAS22, was developed that is applicable to aerodynamic analysis and transonic shock-free redesign of existing two-dimensional cascades of airfoils. CAS22 can be used in three separate modes of operation: (1) as an analysis code for full-potential, transonic, shocked or shock-free cascade flows, (2) as a design code for shock-free cascades that uses Sobieczky's fictitious-gas concept, and (3) as a shock-free design code followed automatically by the analysis in order to confirm that the newly obtained cascade shape provides for an entirely shock-free transonic flow field. CAS22 generates its own four-level, boundary-conforming grid of an O type. The mathematical model of the flow is a full-potential equation. Its artificially time-dependent form is solved in a fully conservative form by using a finite area technique; rotated, type-dependent upstream differencing; and successive line over relaxation. Isentropic shocks are captured by using a first-order artificial viscosity in fully conservative form. The shock-free design is performed by implementing Sobieczky's fictitious-gas concept of elliptic continuation from subsonic into supersonic flow domains. Recomputation inside each supersonic zone is performed by the method of characteristics in the rheograph plane by using isentropic gas relations. The new shock-free contour is determined from the condition that stream functional is equal to zero on the airfoil surface. Besides being capable of converting existing cascade shapes with multiple shocked supersonic regions into shock-free cascades, CAS22 can also unchoke previously choked cascades and make them shock free.			
17. Key Words (Suggested by Author(s)) <b>Shockless design; Transonic flow; Cascade flow; Aerodynamic design; Numerical technique</b>		18. Distribution Statement <b>Unclassified - unlimited STAR Category 02</b>	
19. Security Classif. (of this report) <b>Unclassified</b>	20. Security Classif. (of this page) <b>Unclassified</b>	21. No. of Pages <b>59</b>	22. Price* <b>A04</b>

\* For sale by the National Technical Information Service, Springfield, Virginia 22161